Universidade do Estado do Rio de Janeiro
Centro de Tecnologia e Ciências
Faculdade de Engenharia

Marcos Vinicius dos Santos Issa

On the Accuracy and Efficiency of Cross-Entropy Method for Structural Optimization

Rio de Janeiro
2019

Marcos Vinicius dos Santos Issa

On the Accuracy and Efficiency of Cross-Entropy Method for Structural Optimization

Master's Thesis presented to the Mechanical Engineering Graduate Program of the Universidade do Estado do Rio de Janeiro (UERJ) as a partial requirement to obtain the degree of Master in Sciences.
Field of concentration: Solid Mechanics.

Advisor: Prof. Americo Barbosa da Cunha Junior, DSc
Advisor: Prof. Francisco José da Cunha Pires Soeiro, DSc

Rio de Janeiro
2019

CATALOGAÇÃO NA FONTE

UERJ / REDE SIRIUS / BIBLIOTECA CTC/B

I86 Issa, Marcos Vinicius dos Santos.

On the accuracy and efficiency of cross-entropy method for structural optimization / Marcos Vinicius dos Santos Issa. – 2019.

94f.

Orientadores: Americo Barbosa da Cunha Junior, Francisco José da Cunha Pires Soeiro.

Dissertação (Mestrado) – Universidade do Estado do Rio de Janeiro, Faculdade de Engenharia.

1. Engenharia mecânica - Teses. 2. Otimização estrutural - Teses. 3. Entropia - Teses. 4. Algoritmos genéticos - Teses. 5. Método dos elementos finitos - Teses. I. Cunha Junior, Americo Barbosa da. II. Soeiro, Francisco José da Cunha Pires. III. Universidade do Estado do Rio de Janeiro, Faculdade de Engenharia. IV. Título.

CDU 536.4

Bibliotecária: Júlia Vieira – CRB7/6022

Marcos Vinicius dos Santos Issa

On the Accuracy and Efficiency of Cross-Entropy Method for Structural Optimization

Master's Thesis presented to the Mechanical Engineering Graduate Program of the Universidade do Estado do Rio de Janeiro (UERJ) as a partial requirement to obtain the degree of Master in Sciences.
Field of concentration: Solid Mechanics.

Approved on February 21st, 2019.
Examining Committee:

Prof. Americo Barbosa da Cunha Junior, DSc (Advisor)
Universidade do Estado do Rio de Janeiro

Prof. Francisco José da Cunha Pires Soeiro, DSc (Advisor)
Universidade do Estado do Rio de Janeiro

Prof. Anderson Pereira
Pontifícia Universidade Católica do Rio de Janeiro

Prof. Ivan Fábio Mota de Menezes
Pontifícia Universidade Católica do Rio de Janeiro

Prof. Rodrigo Bird Burgos
Universidade do Estado do Rio de Janeiro

Rio de Janeiro

2019

DEDICATION

I dedicate this, foremost, to God, my mother and the future woman of my life, my bride.

ACKNOWLEDGMENTS

First, I would like to thank God for everything, especially for health and wisdom, because without them I would not complete this stage of my life.

Thank you all my family, but especially my mother Helenice, who always supports me in all my choices and is by my side in all the challenges, making this achievement also her own. Nothing would be possible without you.

Thank you, my bride and future wife Jannaina, my companion whom I am very proud of, my great love. I thank you for the great patience you had with me. I am grateful for all your support, and I would not be able to get here without you.

Thank you, my two advisors. Prof. Soeiro, who since graduation has raised the passion for solid mechanics in mechanical engineering, helping us with very valuable advice, always steering his students in the right direction. And Prof. Americo, who took me out of my comfort zone, made me learn new tools and acquire new knowledge; his relentless pursuit of new knowledge is enviable and is seen as an example. Thank you for your willingness to always help. I am grateful for all your support and advice, which was of much worth.

Thank you to UERJ and all its staff, this institution that I love. I have been at UERJ since I was eight years old when my mother took me there while she was studying Pedagogy. When I graduated from UERJ, I met my fiancée at this beloved institution. That is why I am so fond of this university.

Thank you to everyone who participated in the examining board, who accepted the invitation to evaluate this work. I am grateful for the comments and suggestions of great value for this work.

Finally, thanks Carlos Chagas Filho Research Foundation of Rio de Janeiro State (FAPERJ) under grant E-26/203.155/2016 for the financial support given during these two years of master's program. Thank you very much.

ABSTRACT

ISSA, M.V.S *On the Accuracy and Efficiency of Cross-Entropy Method for Structural Optimization.* 2019. 94 f. Master's Thesis (Master in Mechanical Engineering) – Faculdade de Engenharia, Universidade do Estado do Rio de Janeiro, Rio de Janeiro, 2019.

This dissertation has the objective to evaluate the Cross-entropy method (CE) in structural optimization. Trusses made of tubular structures are used as benchmark tests and it is sought to minimize its mass considering some criteria of structural integrity. The optimal values found by the CE are compared with other results obtained by Sequential quadratic programming (SQP) and Genetic algorithm (GA). Numerical experiments demonstrate that the CE offers a solution for structural optimization in terms of accuracy and efficiency. This dissertation has four structural models where the optimization methods are used considering constraints like yield stress, buckling, natural frequencies, and maximum displacement. For each model, a finite element analysis (FEA) is done to verify the structural integrity criteria which is then used for an optimization problem evaluating the constraints, considering the values found by the three optimization procedures (SQP, GA, CE). In some cases, the optimal values found by the CE are close to those found by the SQP, being SQP a first-order method and CE a zero-order method. The SQP, using the gradient (first-order) in its computational process, is more efficient (better results) and faster than the CE, considering convex problems. When comparing CE with another zero-order method, GA, it is noted that in most cases the CE is faster and has better results than the GA, making the CE quite interesting for application in structural optimization.

Keywords: structural optimization; nonlinear optimization; cross entropy method; optimization experiments.

RESUMO

ISSA, M.V.S *Sobre a Precisão e a Eficiência do Método de Entropia Cruzada para Otimização Estrutural*. 2019. 94 f. Tese de Mestrado (Mestre em Engenharia Mecânica) – Faculdade de Engenharia, Universidade do Estado do Rio de Janeiro, Rio de Janeiro, Brasil, 2019.

Esta dissertação tem como objetivo avaliar o método de entropia cruzada (CE) em otimização estrutural. Treliças compostas por estruturas tubulares são utilizadas como testes de referência e busca-se minimizar a massa em conformidade com os critérios de integridade estrutural. Os valores ótimos encontrados pelo CE são comparados com outros resultados obtidos por programação quadrática sequencial (SQP) e algoritmo genético (GA). Experimentos numéricos demonstram que o CE oferece uma solução para otimização estrutural em termos de precisão e eficiência. São considerados nessa dissertação quatro modelos estruturais onde os métodos de otimização são usados considerando restrições como tensão de escoamento, flambagem, freqüências naturais e deslocamento máximo. Em cada modelo estudado, uma análise de elementos finitos (FEA) é feita para verificar os critérios de integridade estrutural e isto faz parte do problema de otimização, sendo feita quando avalia as restrições, considerando os valores encontrados pelos três métodos de otimização (SQP, GA, CE). Em alguns casos, os valores ótimos encontrados pelo CE são próximos daqueles encontrados pelo SQP, sendo o SQP um método de primeira ordem e o CE é um método de ordem zero. O SQP, utilizando o gradiente (primeira ordem) em seu processo computacional, é mais eficiente (melhores resultados) e mais rápido que o CE, considerando problemas convexos. Ao comparar o CE com outro método de ordem zero, o GA, observa-se que na maioria dos casos, o CE é mais rápido e tem melhores resultados que o GA, tornando o CE bastante interessante para aplicação em otimizaçõ estrutural.

Palavras-chave: otimização estrutural; otimização não linear; entropia cruzada; experimentos em otimização.

LIST OF FIGURES

Figure 1 - BMW Z24 components that were project variables for optimization. . . 18
Figure 2 - Schematic of horizontal drilling 18
Figure 3 - Best platform shape and dimensions of the P-55 platform. 19
Figure 4 - Illustration of the three types of structural optimization. 20
Figure 5 - Schematic classification of several types of metaheuristics methods. . . 28
Figure 6 - Schematic representation of Genetic Algorithm cycle. 29
Figure 7 - Illustration of a generic elastic body subject to prescribed forces and displacements. 31
Figure 8 - Generic distribution with indication γ. 48
Figure 9 - Illustration of objective function with two variables plotted in 3D. . . . 52
Figure 10 - Illustration of objective function with two variables plotted in 2D. . . . 53
Figure 11 - Physical model of the Truss 1. 55
Figure 12 - Contour plot of mass and σ in function of the d_i and H of the Truss 1 with the values found by optimization methods. 59
Figure 13 - Illustration of CE sampling of the domain at different levels (iterations), not considering buckling, of the Truss 1. The magenta cross is the SQP reference solution.(CE control parameters are $N^s = 25$, $N^e = 4$, $\texttt{tol} = 10^{-4}$, $l_{stop} = 13$ and $l_{max} = 100$) 60
Figure 14 - Contour plot of mass, σ_{VM} and σ_E in function of the d_i and H of the Truss 1. 61
Figure 15 - Illustration of CE sampling of the domain at different levels (iterations) considering buckling of the Truss 1. The magenta cross is the SQP reference solution. (CE control parameters are $N^s = 50$, $N^e = 15$, $\texttt{tol} = 10^{-4}$, $l_{stop} = 77$ and $l_{max} = 100$) 62
Figure 16 - Physical model of the Truss 2. 62
Figure 17 - Illustration of CE sampling of the domain at different levels (iterations) of the Truss 2. The magenta cross is the SQP reference solution, not considering buckling. (CE control parameters are $N^s = 25$, $N^e = 3$, $\texttt{tol} = 10^{-4}$, $l_{stop} = 7$ and $l_{max} = 100$) 65
Figure 18 - Illustration of CE sampling of the domain at different levels (iterations) of the Truss 2. The magenta cross is the SQP reference solution considering buckling. (CE control parameters are $N^s = 50$, $N^e = 15$, $\texttt{tol} = 10^{-4}$, $l_{stop} = 40$ and $l_{max} = 100$) 66
Figure 19 - Physical model of the Truss 3. 67
Figure 20 - Physic model of the Truss 4. 74
Figure 21 - Displacements of the Truss 4. 78

LIST OF TABLES

Table 1 - Results found by SQP, GA and CE in a simple objective function without constraint. 52
Table 2 - CE values in each iteration in objective function simple. 54
Table 3 - Stresses at each bar of the two-dimensional truss with nominal conditions in Truss 1. 57
Table 4 - Stress at each bar with values found by optimization methods, not considering buckling, for Truss 1. 58
Table 5 - Comparison between the results obtained with different optimization techniques, not considering buckling, in Truss 1. 58
Table 6 - Stress at each bar with values found by optimization methods considering buckling of the Truss 1. 61
Table 7 - Comparison between the results obtained with different optimization techniques considering buckling in Truss 1. 61
Table 8 - Stresses at each bar in initial conditions of the Truss 2. 63
Table 9 - Comparison between the results obtained with different optimization techniques, not considering buckling, in Truss 2. 64
Table 10 - Stresses at each bar with variables found by SQP, GA and CE method (equals) in Truss 2. 64
Table 11 - Comparison between the results obtained with different optimization techniques considering buckling in Truss 2. 65
Table 12 - Stresses at each bar with variables found by SQP method considering buckling in Truss 2. 66
Table 13 - Stresses at each bar with variables found by GA method considering buckling in Truss 2. 66
Table 14 - Stresses at each bar with variables found by CE method considering buckling in Truss 2. 66
Table 15 - Stresses at each bar in nominal conditions in Truss 3. 68
Table 16 - Comparison between the results obtained with different techniques optimizing the area of each bar in Truss 3. 68
Table 17 - Values at each bar with variables found by SQP method in Truss 3. . . . 68
Table 18 - Values at each bar with variables found by GA method in Truss 3 . . . 69
Table 19 - Values at each bar with variables found by CE method in Truss 3. . . . 69
Table 20 - Illustration of the areas obtained by the three optimization methods considering yield stress constraint in Truss 3. 69
Table 21 - Natural frequencies in the Truss 3 with nominal parameters in Hz. . . . 70

Table 22 - Comparison between the results obtained with different techniques optimizing the area of each bar in Truss 3. 71
Table 23 - Values of cross-sectional area in the Truss 3 found by optimization methods in mm^2. 71
Table 24 - Illustration of the areas obtained by the three optimization methods considering natural frequencies constraint in Truss 3. 71
Table 25 - Natural frequencies in the Truss 3 found by optimization methods in Hz. 71
Table 26 - Comparison between the results obtained by CE, HS and FA optimizing the area of each bar in Truss 3. 72
Table 27 - Values of cross-sectional area in the Truss 3 found by optimization methods CE, HS and FA in mm^2. 72
Table 28 - Illustration of the areas obtained by CE, HS and FA considering natural frequencies constraint in Truss 3. 73
Table 29 - Natural frequencies in the Truss 3 found by optimization methods CE, HS and FA in Hz. 73
Table 30 - Stresses at each bar in initial conditions in Truss 4. 75
Table 31 - Comparison between the results obtained with different optimization techniques, not considering buckling, optimizing d_i, t, h_1 and h_2 in Truss 4. 75
Table 32 - Stresses at each bar with variables found by SQP method, not considering buckling, optimizing d_i, t, h_1 and h_2 in Truss 4. 75
Table 33 - Stresses at each bar with variables found by GA method, not considering buckling, optimizing d_i, t, h_1 and h_2 in Truss 4. 76
Table 34 - Stresses at each bar with variables found by CE method, not considering buckling, optimizing d_i, t, h_1 and h_2 of the Truss 4. 76
Table 35 - Comparison between the results obtained with different optimization techniques considering buckling and optimizing d_i, t, h_1 and h_2 of the Truss 4. 76
Table 36 - Stresses at each bar with variables found by SQP method considering buckling and optimizing d_i, t, h_1 and h_2 in Truss 4. 77
Table 37 - Stresses at each bar with variables found by GA method considering buckling and optimizing d_i, t, h_1 and h_2 in Truss 4. 77
Table 38 - Stresses at each bar with variables found by CE method considering buckling and optimizing d_i, t, h_1 and h_2 in Truss 4. 77
Table 39 - Displacements in each node of the Truss 4 in nominal conditions. . . . 78
Table 40 - Comparison between the results obtained with different optimization techniques subject to maximum displacement optimizing d_i, t, h_1 and h_2 in Truss 4. 78

Table 41 - Displacement of each node in mm using the values found by the optimization methods of the Truss 4. 78
Table 42 - Values of objective function and Func. Eval. obtained by SQP, not considering buckling, in Truss 1. 89
Table 43 - Values of objective function and Func. Eval. obtained by GA for several values of `tol`, p_e and Ps, not considering buckling, in Truss 1. 90
Table 44 - Values of objective function and Func. Eval. obtained by CE for several values of `tol`, ϱ and N^s, not considering buckling, in Truss 1. 91
Table 45 - Objective functions optimal obtained by SQP considering buckling in Truss 1. 92
Table 46 - Values of objective function and Func. Eval. obtained by GA for several values of `tol`, p_e and Ps considering buckling in Truss 1. 93
Table 47 - Objective functions optimal obtained by CE for several values of `tol`, ϱ and N^s, not considering buckling, in Truss 1. 94

LIST OF ABBREVIATIONS AND ACRONYMS

SQP	Sequential Quadratic Programming
GA	Genetic Algorithm
BFGS	Broyden-Fletcher-Goldfarb-Shanno
DFP	Davidon-Fletcher-Powell
GRASP	Greedy Randomized Adaptive Search Procedure
PSO	Particle Swarm Optimization
CE	Cross Entropy Method
DNA	Deoxyribonucleic acid
FEA	Finite Elements Analyses
FBD	Free Body Diagram
CPU time	Time of central processing unit
Func. Eval.	Function evaluation
HS	Harmony Search
FA	Firefly Algorithm

LIST OF SYMBOLS

$\boldsymbol{n}$	Normal vector
$\boldsymbol{u}$	Displacement field
$\boldsymbol{\sigma}$	Stress tensor
$\boldsymbol{\epsilon}$	Strain tensor
$\mathcal{C}$	tensor of elasticity
$\mathbf{t}$	Force vector prescribe in $\mathfrak{B}$
Γ_D	the partition of $\partial\mathfrak{B}$ on which the displacements are prescribed
Γ_N	the partition of $\partial\mathfrak{B}$ on which the forces $\boldsymbol{t}$ are prescribed
w	Weight function
∇f	Gradient of f
V	Volume
$[\mathbf{K}]$	Stiffness matrix
$[\mathbf{M}]$	Mass matrix
$\mathbf{U}$	Displacement vector
u_n	Horizontal displacement in node n
v_n	Vertical displacement in node n
$\mathbf{F_r}$	Force vector
$\mathbf{f_{rD}}$	Force value in degree freedom D
S_Y	Yield stress
σ_{VM}	Von Mises criterion
σ^E	Buckling stress
E	Young's modulus
I	Moment of inertia
L	Length
A	Cross area
N	Elements number
n	Nodes number
D	Degree freedoms number
L_e	Element length
$[\overline{\mathbf{K}}_e]$	Elementary stiffness matrix in global coordinates
$[\overline{\mathbf{M}}_e]$	Elementary mass matrix in global coordinates
ω	Natural frequency
ω^*	Natural frequency used as constraint
d_p	Displacement
$d_{p_{max}}$	Maximum displacement
θ	Angle formed between the bar longitudinal and the horizontal

P	Load applied
B	Base half the first structure model
ρ	Density
H	Height
d_i	Internal diameter
d_e	External diameter
t	Thickness
$\mathcal{N}$	Normal force in the bar
θ	Angle the first structure model.
m	Structure mass
$\mathbf{B}_e$	Deformation matrix
$\mathbb{R}^n$	The n-dimensional Euclidian space
$\mathcal{J}$	objective Function
$\hat{\mathcal{J}}$	objective Function estimator
$\boldsymbol{x}$	Vector of Variables
p_i	Constraints with equality
q_j	Constraints with inequality
$\mathcal{A}_{adm}$	Conditions for generic formulation of an optimization problem
∂	Derivative partial
$\mathcal{L}$	Lagrangian
λ	Lagrange multipliers
$\mathcal{H}$	Hessian
e	Euler number
$\mathcal{J}_{adap}$	Adaptive function
$\mathbb{X}$	Real value
X^l	The minimum real value
X^u	The maximum real value
X^{bin}	Current binary
ϖ_i	Measure of adaptability
φ	Number of binary digits
Ps	Population size in GA
p_e	Percentage of the population size used in the elite count
A_c	Continuous variable accuracy
Ω	Sample space
Σ	Set of all relevant events
$\mathcal{P}$	Measure probability
X	Random variable
F	Probability distribution of function
f	Probability density of function

$\mathbb{E}\{X\}$	Expectation of the random variable X
μ	Mean value
s	Standard deviation
$\boldsymbol{X}$	Vector with random variables
ℓ	Probability of estimation
$f(\boldsymbol{X})$	PDF of the continuous random vector $\boldsymbol{X}$
$g(\boldsymbol{X})$	PDF of the continuous random vector $\boldsymbol{X}$ which $g(\boldsymbol{x}) = 0$
$\hat{\ell}$	Unbiased importance sampling estimator of ℓ
$\mathcal{D}$	Kullback-Leibler divergence
Var	Variance
g^*	Optimal importance sampling density
h	Chosen probability density of importance
h^*	Optimal probability density of importance
$\boldsymbol{v}$	Reference parameter vector
$\boldsymbol{v}^*$	Optimal reference parameter vector
W	Likelihood ratio
$\mathbb{1}$	Indicator function
ti	Iteration number
γ	Level indication in generic distribution
$\hat{\boldsymbol{v}}$	Reference parameter estimator
$\hat{\gamma}$	Level indication estimator
γ^*	Level indication in generic distribution optimal
ϱ	Quantile of performance values
N^s	Sample size
N^e	Number of elite samples
ν_i	Measures the importance of the ith penalty
`tol`	Tolerance
α	Smoothing constant
β	Large smoothing constant
ϑ	Small integer in large smoothing
l_{stop}	CE stop iteration
l_{max}	CE maximum iteration
m_{ad}	Added mass

SUMMARY

	INTRODUCTION	17
1	**LITERATURE REVIEW**	24
1.1	**Structural optimization**	24
1.2	**Generalities on optimization theory**	25
1.3	**Gradient-based methods**	26
1.3.1	Steepest descent	26
1.3.2	BFGS algorithm	26
1.3.3	DFP formula	27
1.3.4	Sequential quadratic programming	27
1.4	**Metaheuristic methods**	27
1.4.1	Genetic Algorithm	28
1.4.2	Particle swarm optimization	29
1.4.3	Simulated annealing	30
1.5	**Cross-entropy method**	30
2	**OPTIMIZATION IN SOLID MECHANICS**	31
2.1	**Balance equations from continuum mechanics**	31
2.2	**Discretization of balance equations**	32
2.3	**Criteria for structural integrity**	33
2.3.1	The von Mises yield criterion	34
2.3.2	Buckling	35
2.4	**Structural optimization**	35
2.5	**Finite element analysis**	36
3	**NUMERICAL METHODS**	39
3.1	**Generic formulation of an optimization problem**	39
3.2	**Sequential quadratic programming**	40
3.3	**Genetic algorithm**	41
3.3.1	Selection	43
3.3.2	Crossover	43
3.3.3	Mutation	43
3.4	**Cross-entropy method**	44
3.4.1	Importance sampling estimator	45
3.4.2	Kullback-Leibler divergence	46
3.4.3	Rare-event probability estimation	47
3.4.4	Cross-entropy algorithm for rare-event estimation	49
3.4.5	Cross-entropy algorithm for optimization	49
3.5	**Example with a simple function**	51

4 **NUMERICAL EXPERIMENTS** 55
4.1 **Truss 1 - 2 bars and 3 nodes** 55
4.1.1 Optimization with yield stress constraint 58
4.1.2 Optimization with yield stress and buckling limit constraints 60
4.2 **Truss 2 - 11 bars and 6 nodes** 62
4.2.1 Optimization with yield stress constraint 63
4.2.2 Optimization with yield stress and buckling limit constraints 65
4.3 **Truss 3 - 10 bars with 6 nodes** 67
4.3.1 Optimization of cross-sectional areas with yield stress constraint 68
4.3.2 Optimization with natural frequency constraints 69
4.4 **Truss 4 - 15 bars and 8 nodes** 74
4.4.1 Optimization with yield stress constraint 75
4.4.2 Optimization with yield stress and buckling limit constraints 76
4.4.3 Optimization subject to maximum displacement 77
CONCLUDING REMARKS 80
REFERENCES 82
APPENDIX A – Parameter analysis - Truss 1 89

INTRODUCTION

In this chapter, a general introduction for this dissertation is presented. It includes a motivation for the addressed research problem, the underlying scientific and technological challenges, the objectives of the work and the manuscript outline.

Optimization in engineering

Projects, constructions, and maintenance require engineers and managers to manage decisions at various stages. Optimization methods are tools used in several phases in the decisions management. (RAO, 2009).

This need for optimization in engineering is evident in the design of a new product and also in the modification of the design of an existing product. Performing this task is not simple, mainly due to the many options that the designer has at his disposal (VENKATARAMAN, 2002).

The approach traditionally adopted in various industry sectors employs a trial and error methodology. This procedure chooses new settings based primarily on the professional experience. However, the choice of a new design is often not obvious, because it works with conflicting objectives, such as reducing mass and increasing durability simultaneously. Thus, satisfactory but not optimal products or processes are generally obtained (YANG, 2010).

In order to develop better and cheaper products, professionals are committed to the optimization methodology since it employs a scientic method of faster searching capabilities. This methodology uses a mathematical optimization algorithm as an element to select new designs iteratively in search of optimum configuration (SHUKLA; TIWARI, 2005).

To begin applying engineering optimization techniques, it is necessary to define some basic objects: objective functions, design variables and constraints. Design variables are the parameters free to modify, for example, geometric variables (thickness, width, radii of curvature, etc), operating variables (input speed, load, temperature, etc) and other quantities such as materials, trajectories, etc. The objective functions define the goals of the project, that are, to minimize or maximize variables such as efficiency, costs, stresses, load loss, friction, thermal exchange, etc. These functions are the driving forces of optimization. Finally, constraints are the requirements that must be met by the new designs. They can be requirements coming from standards, feasibility or manufacturing (MUSKULUS; SCHAFHIRT, 2014).

As an example of the optimization success, consider the BMW Team competition car in the Interlagos race during the GT3 Championship. In order to reduce the lap time (objective function), several car setup parameters have been modified: angle of the aerofoil, configuration of the shock absorbers, wheels, among others. In total, 600 different simulations were run in just one day, obtaining in the end a reduction of 1.38 seconds per lap. A significant improvement for this competition (HORCAIO, 2013).

Figure 1 - BMW Z24 components that were project variables for optimization.

Source: (HORCAIO, 2013)

Within the oil and gas industry, an article (CUNHA Jr; SOIZE; SAMPAIO, 2015) and a thesis (CUNHA Jr, 2015) show the search for a optimal configuration for the operating parameters (weight on bit and column rotation) of an oil well drilling column, aiming to maximize the advance speed of the column in the soil, reduce the production time of the well and to reduce resource costs in the operation. A schematic of horizontal drilling is presented in Figure 2.

Figure 2 - Schematic of horizontal drilling

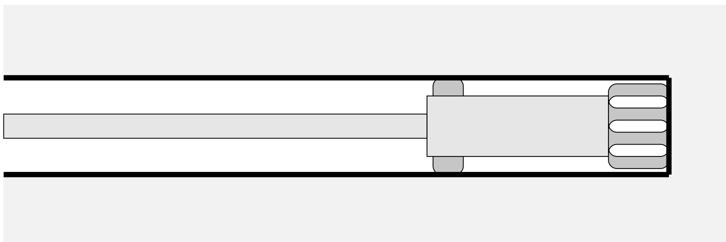

Source: (CUNHA Jr; SOIZE; SAMPAIO, 2015)

Still in the context of the oil and gas industry, Petrobras used optimization to perform the initial design of the P-55 platform, which is the largest semi-submersible platform built in Brazil and already is in operation. The objective was to find the dimensions of the hull of the platform that minimizes the vertical movement and comply with various design constraints, such as movement, construction, and assembly (OLIVEIRA, 2008). The nature of the problem and the constraints have greatly reduced the number of viable configurations, so it was necessary to use a robust optimization algorithm capable of finding the viable regions. The studies included hydrodynamic, stability and fatigue analysis. A schematic of P-55 platform is presented Figure 3.

Figure 3 - Best platform shape and dimensions of the P-55 platform.

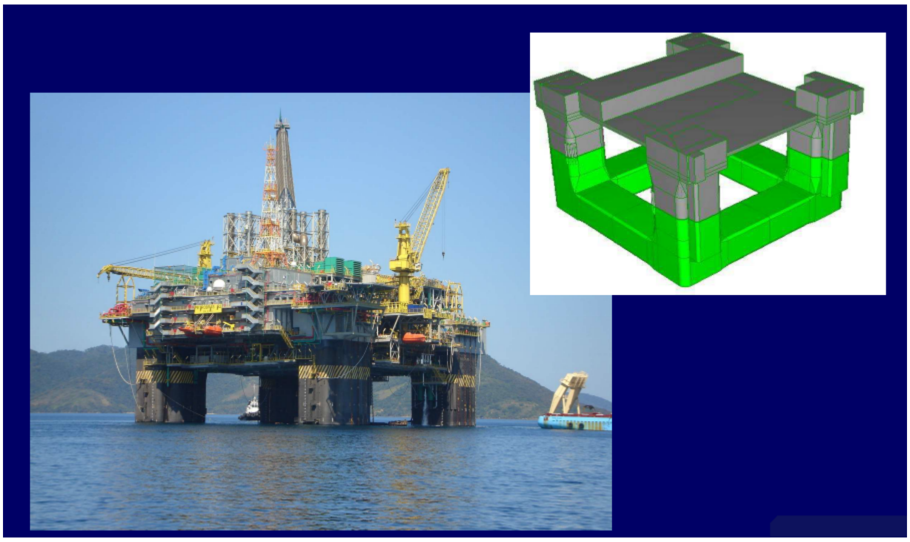

Source: (OLIVEIRA, 2008)

Structural optimization

Structural optimization (CHRISTENSEN; KLARBRING, 2009) seeks a better performance of the structure, which means that it meets the mechanical demands that the structural component is expected to provide using less material, reducing mass and consequently reducing the weight. It consists in minimizing the weight while still meeting the criteria of structural integrity. Due to complex geometric and the use of advanced materials, which have extremely nonlinear behavior, this can be very challenging (SAITOU et al., 2005; ZAVALA et al., 2014).

Structural optimization has been applied to the development of industrial problems for several years, with several types of materials. There are three types of optimization structural problems: sizing, shape, and topology (CHRISTENSEN; KLARBRING, 2009; GHASEMI; DIZANGIAN, 2010; SOUZA et al., 2016).

Figure 4 - Illustration of the three types of structural optimization.

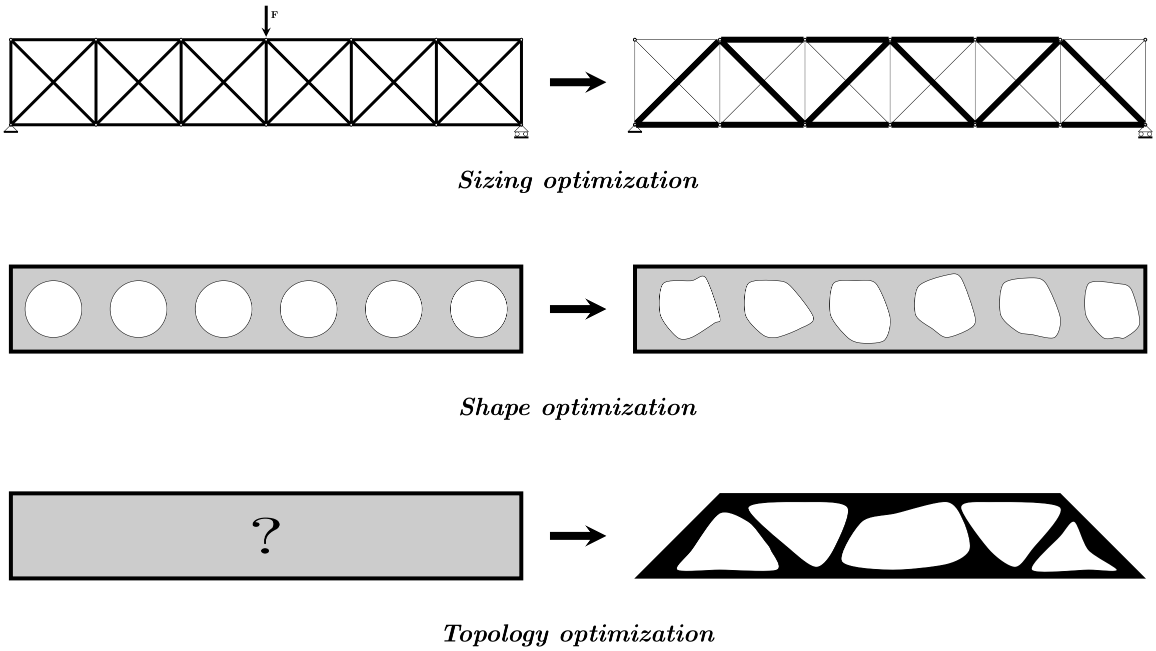

Sizing optimization changes the size, such as cross-sections and other internal dimensions of structural components. The performance of structures can be improved by optimal cross-sections. This may result in improved structural stiffness while decreasing structural weight. For this reason, it is very common in the aircraft industry in the components of the airplanes (CAVAGNA S. RICCI, 2011; GRIHON, 2017).

Shape optimization achieves the ideal shape modifying the predetermined boundaries. For a truss, the design variables change the node positions. This type of optimization can be used to improve impact resistance or the welding process (EBY et al., 2002; BOGOMOLNY; BENDSOE; HATTEL, 2009).

Topology optimization is frequently applied in structural optimization. All definitions are based on a model analysis. The final result is the optimal material distribution. One can cite as an example the topological optimization of a structure to improve the passage of air or simply to improve flow efficiency (DEATON; GRANDHI, 2014). There are examples too in the automotive industry (CAVAZZUTI et al., 2010) and other areas (TALISCHI et al., 2010; VATANABE et al., 2016; CHUN; SONG; PAULINO, 2019; SANDERS; AGUILÓ; PAULINO, 2018; CUELLAR et al., 2018; THEDIN et al., 2018).

Scientific and technological challenges

Optimization is intrinsically tied in achieving the highest overall performance, whether one is an athlete, artist, engineer, economist (DANILO; GIRALDO, 2017) or computer scientist (CHAOVALITWONGSE et al., 2017). Normally, computer analysis is used to evaluate the quality of projects, with computational codes for calculation. Finite element analysis (FEA), for example, is performed to calculate displacements, stresses, vibration frequencies and other quantities of a structure. In a more general setting, computational tools and sometimes experiments are constructed to judge the quality of the proposed designs (VANDERPLAATS, 2006; ZAVALA et al., 2014).

If not satisfactory, the design is modified and analyses are repeated to improve the product attending the design requirements. This approach of analysis and revision involves changing variables. One can change many of design parameters simultaneously to improve the design while verifying if all design constraints are met. The numerical optimization does this. However, one of the difficulties is adapting the numerical methods for each problem, which sometimes may become costly and prohibitive. (HAFTKA; GRANDHI, 1986; VANDERPLAATS, 2006).

The development of equipment, product or structure must have a good balance between cost, time and quality. As the complexity of developed products increase, the list of relevant resources become extensive and the deadlines for completing projects get shortened. In the face of these challenges, the numerical methods present themselves as a useful tool.

Due to the discontinuities and geometric complexity of some structural models, derivative or gradient based methods may not possible to be used. Metaheuristics methods are important in structural optimization because, usually, they too do not need the gradient of the objective function in the optimization problem. In addition, new metaheuristics methods are emerging (LAGAROS; PAPADRAKAKIS; KOKOSSALAKIS, 2002; OFTADEH; MAHJOOB; SHARIATPANAHI, 2010; MIGUEL; MIGUEL, 2012; LIANG; JUAREZ, 2015) and they are efficient algorithms which made it possible to find the optimum solutions of engineering problems (LEE; GEEM, 2005).

However, in some cases metaheuristic techniques bring great computational cost, which may be prohibitive. Despite the successful applications of metaheuristics in finding optimal solutions to structural design problems, there are examples where metaheuristic optimization methods are criticized on the basis of having no mathematical background. Moreover, in two articles (WEYLAND, 2010; SORENSEN, 2013) some of the metaheuristics are not new being imitation of other metaheuristics. In one article, it is even suggested that researchers should be cautioned to conduct research on metaheuristics (SAKA; HASANCEBI; GEEM, 2016). It is a great challenge to develop computationally efficient metaheuristics.

The great technological and scientific challenge is to develop increasingly efficient, effective and robust computational methods to solve increasingly complex problems, surpassing the previously mentioned problems, such as discontinuities and geometric complexity. Advanced and well-developed computational methods are a requirement to solve different types of problems, because only some methods, as metaheuristics for example, may solve some problems with a certain amount of efficiency and effectiveness. The solution of complicated optimization problems where classical numerical methods (gradient-based) are not applicable is a common necessity, and the main alternatives in this case are the metaheuristics, which are computationally more expensive.

Problem definition and objectives

In the context defined in the previous section of this dissertation, the objective is the development of a new framework to deal with the structural optimization problem that employs the Cross-entropy Method (CE) (RUBINSTEIN, 1999; RUBINSTEIN, 2001; BOER et al., 2005; KROESE et al., 2013), a Monte Carlo technique (KROESE; TAIMRE; BOTEV, 2011; RUBINSTEIN; KROESE, 2017) developed for the simulation of rare events and frequently used in combinatorial optimization. To the best of the author's knowledge, there is only one work where this optimization method is used in structural optimization (GHIDEY, 2015).

The specific objectives of this dissertation are to present a theoretical formulation where CE is used as a numerical tool, showcasing implementation of this method in a computational library and to evaluate the new methodology regarding accuracy and computational efficiency when compared with other classical methods.

Dissertation contributions

This dissertation is focused on proposing a new computational framework for structural optimization based on the Cross-entropy method, a relatively new metaheuristic that is successfully used in the simulation of rare events and combinatorial optimization. In this context, the work presents as contributions: (i) the development of the mathematical formalism necessary to state the problem of structural optimization, as well as the analysis of the new numerical procedure; (ii) the implementation of the new numerical method in a computational code written in MATLAB language; (iii) a detailed analysis on the accuracy and efficiency of this new framework.

Manuscript organization

This manuscript is divided in four chapters. Chapter 1 presents a review of the scientific literature addressing structural optimization challenges and optimization techniques employed in this area. Chapter 2 presents the solid mechanics concepts used by structural optimization. Chapter 3 introduces mathematical formulation of a general optimization problem and discusses about numerical techniques of optimization methods that are applied in this dissertation. Numerical experiments are presented in chapter 4, as well as a proper discussion.

1 LITERATURE REVIEW

This chapter presents a literature review related with structural optimization problems, optimization methods and an introduction to metaheuristic methods employed in this scenario.

1.1 Structural optimization

The concept of optimization is tied to natural phenomena. Sir George Cayley (1773-1857) measured the shape of a trout and noted, without mathematical proof, that the trout has the form ideal to minimize flow resistance. Theodore von Karman observed that this is precisely the shape of a lowdrag airfoil. Oliver Wendell Holmes (1809-1894), in his classic verse, "The Deacon's Masterpiece or The Wonderful OneHoss Shay," recorded man's desire to produce a uniformly strong, durable product. Perhaps the first structural optimization was done by Maxwell in 1869, and then by Michel in 1904 on a more famous work. These works supplied theoretical lower bounds on the weight of trusses and offer considerable insight into the structural optimization problem (VANDERPLAATS, 1982).

Since then, the improvement of techniques for structural optimization has been constantly sought, and currently greater computational resources are at disposal for scientific and technological advance. There is a continuous development of new methods, especially metaheuristics. One is always looking for the development of structural optimization methods by the shape (HSU, 1994; AKBARI; SADOUGHI, 2013), size (BEKDAS S. M. NIGDELI, 2015) and topology (CHUN; SONG; PAULINO, 2019). A work of Sanders (SANDERS; AGUILÓ; PAULINO, 2018) stands out, which uses a topological structural optimization with multimaterials that demonstrate the amount of variables that may be worked with.

In the mechanical engineering department of the Unversidade do Estado do Rio de Janeiro there are recent dissertations dealing with structural optimization. Two more recent works can be mentioned: the dissertation of Lopes (LOPES, 2017) and Mendonça (MENDONÇA, 2017). Another related dissertation dealing with structural optimization is the work of Yilmaz (YILMAZ, 2014), which regards structural optimization of offshore wind turbine towers. Other relevant dissertations can be found in (ZHANG, 2014; SILVA, 2016; BRUNO, 2017; ROCHA, 2017).

1.2 Generalities on optimization theory

The discrete optimization problem has unknown variables of a finite set. Discrete optimization problems can contain not only integer or binary variables, but also abstract variable such as permutations. On the other hand, the viable set for continuous optimization problems is usually uncountable. Continuous optimization problems are usually easier to solve because it is possible to use objective functions and constraints at a given point and get information about the behavior of the function at all points close to the desired value (RAJEEV; KRISHNAMOORTHY, 1992; NOCEDAL; WRIGHT, 2006).

Continuous optimization techniques have an important role in solving discrete optimization problems. For example, the branch-and-bound method (MOHAMED et al., 2007; RASTI-BARZOKI; HEJAZI; MAZDEH, 2013) for integer linear programming problems request the repeated solution. These subproblems are frequently solved by the Simplex method (MAROS, 2013; NOCEDAL; WRIGHT, 2006).

Optimization problems can be classified according with the number of variables, functions smoothness (differentiable or nondifferentiable), objective function, constraints (linear, nonlinear, convex, not convex) and other characteristics (RAO, 2009).

Unconstrained optimization problems arise in many practical applications. It may be safe to disregard some restrictions because they do not affect the solution and do not interfere with the algorithms, even for some problems with natural constraints. Unconstrained problems also come from reformulated constrained optimization problems where the constraints are substituted by penalization terms added to objective function. This remove the constraints violations (NOCEDAL; WRIGHT, 2006; BONNANS et al., 2009; RAO, 2009).

Constrained optimization problems come from models in which the constraints limit the resolution of optimization problems. If objective function and constraints are linear functions, the optimization problem will be a linear programming problem. Linear programming problems are the most widely formulated and solved of all optimization problems, for example, in management, financial, and economic applications. Nonlinear programming problems, where at least some of the constraint or the objective function are nonlinear, are natural in the physical sciences, engineering, management and economic sciences (NOCEDAL; WRIGHT, 2006; BONNANS et al., 2009; RAO, 2009).

The global solution is needed in some applications, but in many problems it is difficult to find. Sometimes one does not find the global solution. For convex programming and linear problems, the local solution is the global solution. Nonlinear problems, unconstrained and constrained, may have a local solution, not global (NOCEDAL; WRIGHT, 2006).

A "good algorithm" for numerical optimization must have these characteristics:

- Robustness. Should have the same performance in several types of problems of the same group, independent of the value chosen for the starting point.

- Efficiency. Should not require too much time and computational storage
- Accuracy. Should find solutions precisely, not being sensitive to data errors and arithmetic rounding.

These characteristics are conflicting. Robust methods may also be slow. A fast convergence method for a unconstrained nonlinear problem may need too much computer storage. Trade-offs between convergence rate and storage, between robustness and speed, so on, are central points in numerical optimization (NOCEDAL; WRIGHT, 2006). The choice of one of these optimization methods depends on the type of design variables and the time available for optimization.

1.3 Gradient-based methods

A gradient-based method is a numerical tool to find the local minimum of a function using the search directions defined by the gradient (maximum decline). Methods which require the gradient with respect to all parameters to be computed are called first-order methods (BONNANS et al., 2009). Some types of gradient-based optimization methods are Steepest Descent, BGFS algorithm, DFP formula and Sequential quadratic programming.

1.3.1 Steepest descent

Steepest descent is a gradient-based optimization method. Optimization methods, which use the gradient vector to define the search direction for each iteration, are known first-order methods because they use first-order partial derivatives of a function. The simplest and most famous of these methods is the steepest descent, proposed by Cauchy in 1847 (YUAN, 2006; SNYMAN; WILKE, 2018).

1.3.2 BFGS algorithm

Broyden–Fletcher–Goldfarb–Shanno (BFGS) algorithm is a method for unconstrained nonlinear optimization problems. BFGS is a quasi-Newton method. The quasi-Newton method is an alternative to Newton's method that seek a point of a objective function twice differentiable. Newton's method and BFGS methods are not ensured to converge, unless the objective function has a quadratic Taylor expansion close an optimum point. BFGS has a good performance for non-smooth optimizations (BROYDEN, 1970;

FLETCHER, 1970; GOLDFARB, 1970; SHANNO, 1970).

1.3.3 DFP formula

Davidon–Fletcher–Powell formula (DFP; William Davidon, Roger Fletcher, and Michael Powell) finds the solution of the secant equation that is nearest to the solution estimated and satisfies the curvature condition. DFP was the first quasi-Newton method that generalized the secant method to multidimensional problems. DFP keeps the symmetry and positive definiteness in the Hessian matrix. A Hessian matrix is a quadratic matrix with second-order partial derivatives. It represents the function curvature. Hessian matrices are used commonly in problems that do not use Newtonian methods (DAVIDON, 1991; AL-BAALI; FLETCHER, 1986; FLETCHER; MAZA, 1989; NOCEDAL; WRIGHT, 2006; BONNANS et al., 2009; FLOUDAS; PARDALOS, 2009).

1.3.4 Sequential quadratic programming

The Sequential Quadratic Programming (SQP) algorithm is a form of Newton's method to solve problems adapted to computation. SQP is one of the most used techniques for nonlinear constrained optimization generating steps by solving quadratic subproblems. This SQP approach may be used both in line search and trust-region frameworks (BOGGS; TOLLE, 2000; NOCEDAL; WRIGHT, 2006; BONNANS et al., 2009).

1.4 Metaheuristic methods

Metaheuristic methods are used to solve generic optimization problems, generally applied to problems for which no efficient algorithm is known. They are general algorithmic structures adaptable to various optimizations, using a combination of random choices and historical knowledge of old results acquired by the method to guide their searches in neighborhoods within the research space, which avoids premature stops. Methods which use only the criterion value at some positions and do not rely on derivatives are called zero-order methods (or derivative-free) (BONNANS et al., 2009). There are several types of metaheuristics and classifications, as shown in Figure 5. In the classification of metaheuristics, there are those inspired by nature and populations. Within these, one has evolutionary algorithms like Genetic Programming, Differential Evolution, Particle Swarm Optimization, Estimation of Distribution Algorithm and Simulated Annealing. The ones inspired by trajectories are GRASP (Greedy Randomized Adaptive Search Procedure), Variable Neighborhood Search, among others. Other classifications can be seen in Figure 5. New metaheuristic methods are constantly being created to solve specific problems, and thus new classifications arise.

Figure 5 - Schematic classification of several types of metaheuristics methods.

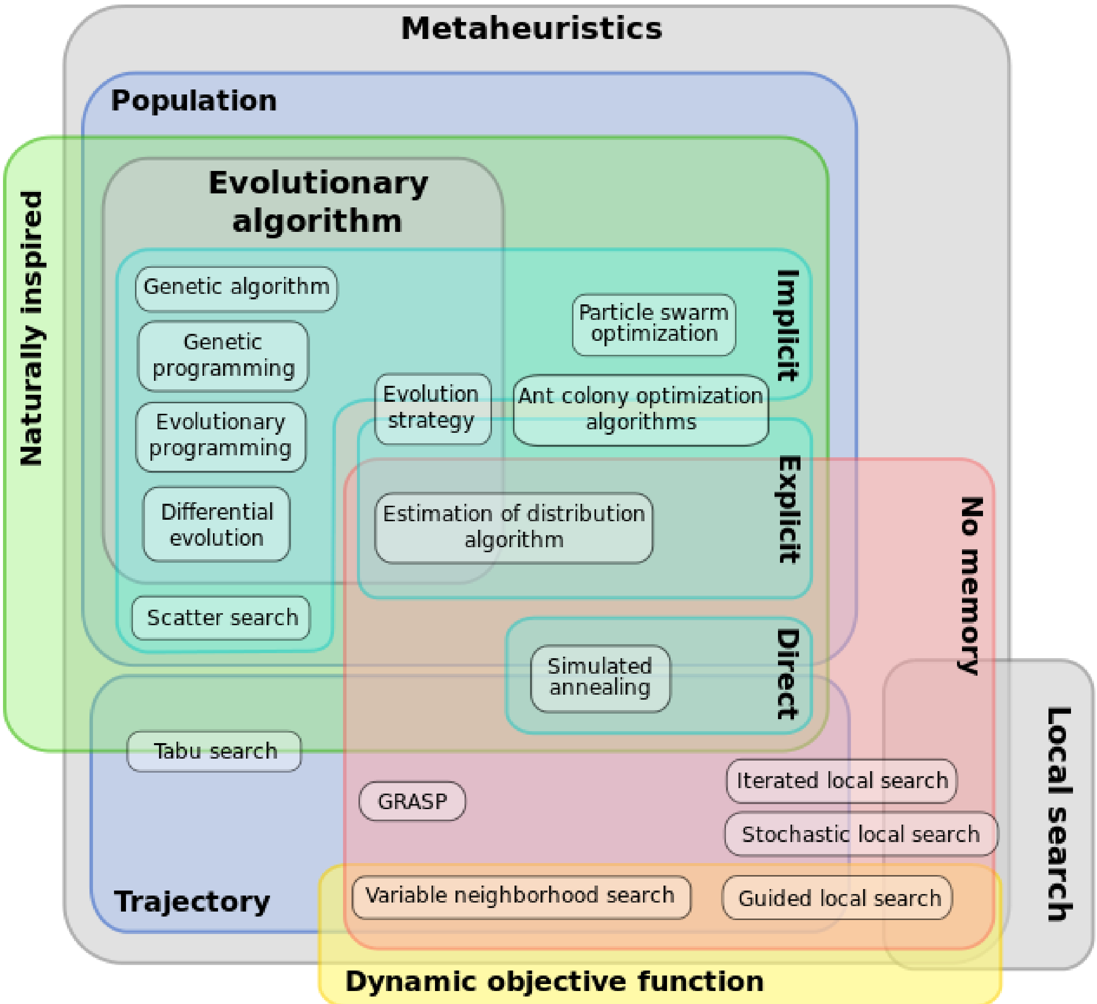

Source: https://en.wikipedia.org/wiki/Metaheuristic

1.4.1 Genetic Algorithm

Genetic Algorithms (GA) are based on the biological concept of evolution in the algorithmic recipes. As GA is part of many intelligent systems, it is also frequently considered in the areas of computational intelligence and artificial intelligence (KRAMER, 2017).

The Figure 6 shows the continuous cycle of artificial evolution that is inspired by natural evolution. The evolutionary process begins with randomly or manual solutions.

Figure 6 - Schematic representation of Genetic Algorithm cycle.

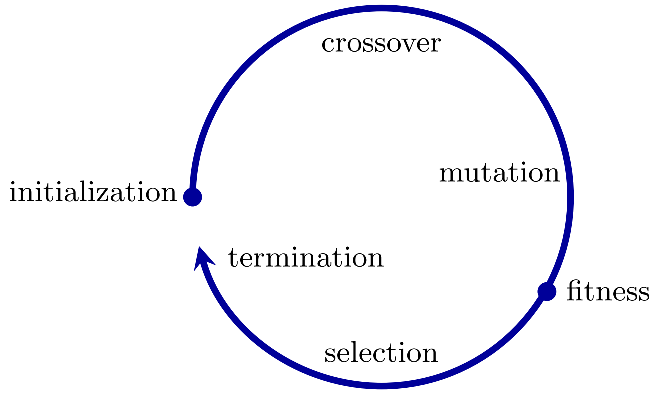

In according wtih Goldberg (GOLDBERG, 1989), these algorithms combine the fitting with randomized information exchange to form new algorithms. In each generation, a new group of artificial creatures (strings) are created using parts of the fittest ones between the old, while the new part is tested for good measure.

GA operates on string populations, with the string encoded to represent some underlying set of parameters. Reproduction, cross-over and mutation apply successive copies of ex-strings and strings. However, despite its simplicity, the resulting research performance is broad. GA performs an innovative exchange of concepts between strings and thus connects to our own research or discovery ideas.

Four steps separate GA from more conventional optimization techniques:

1. Direct manipulation of a coding,
2. Search from a population,
3. Search via sampling,
4. Search using stochastic operators.

1.4.2 Particle swarm optimization

Particle Swarm Optimization (PSO) is inspired in social and cooperative behavior exhibited by various species such as birds and fishes. It was created by Russell Eberhart and James Kennedy in 1995 (KENNEDY; EBERHART, 1995). Originally, the two began developing software simulations inspired in birds flocking around foods. PSO may be applied in structural optimization (PEREZ; BEHDINAN, 2007) and even in photovoltaic solar system (KHARE; RANGNEKAR, 2013).

1.4.3 Simulated annealing

Simulated Annealing is a metaheuristic optimization method consisting in a probabilistic local search technique. It is an iterative stochastic search method that has inspiration in the annealing of the physical metallurgy, that involves a heating and a controlled cooling of a material, reducing the defects and increasing mechanical strength and hardness (HADDOCK; MITTHENTAL, 1992). As an example, simulated annealing can be applied in deep learning (RERE; FANANY; ARYMURTHY, 2015), solution of an inverse radiative transfer problem (SILVA NETO; SOEIRO, 2006) and structural optimization (LEITE; TOPPING, 1999).

1.5 **Cross-entropy method**

The CE has its origins in an adaptive algorithm for rare-event simulation, based on variance minimization, that uses Kullback–Leibler divergence as a measure of proximity between two sampling distributions (BOTEV et al., 2013). It was proposed first time by Rubinstein (RUBINSTEIN, 1997). The CE is modified to an algorithm for rare-event estimation and combinatorial optimization where the original variance minimization program is replaced by a similar CE minimization program.

The CE is a Monte Carlo technique for estimation and optimization problems. Monte Carlo techniques are used for computational generation of random objects (KROESE et al., 2014). This method can be used for two types of problems: estimation and optimization (BOTEV et al., 2013). The CE was applied to the estimation of probability of rare events in dynamic models (RUBISTEIN; KROESE, 2004).

The CE has already been applied in combinatorial optimization and estimation of rare events. Application areas include DNA sequence alignment, telecommunication system queuing models, neural computing, control and navigation, signal processing, programming, project management, and reliability systems (KROESE; POROTSKY; RUBINSTEIN, 2006).

The CE also is connected to the fields of neural computing and was also successfully applied in vector grouping and quantization. It can be considered that the CE is a stochastic algorithm with two iterative phases: generation of random samples and update of the random parameters, as parameters of probability density function (RUBINSTEIN; KROESE, 2017).

The CE concept defines a precise mathematical framework that provides fast and “good” update / learning rules (BOER et al., 2005; KROESE; POROTSKY; RUBINSTEIN, 2006; RUBINSTEIN; KROESE, 2017).

2 OPTIMIZATION IN SOLID MECHANICS

In this chapter, the balance equations from continuum mechanics as well as suitable boundary conditions are presented to construct a physical-mathematical model for the structural problem of interest. A generic formulation is made to propose a framework for application in general, although this dissertation only analyzes trusses. The criteria for structural integrity and the calculation of the mass of the structure are also introduced in this dissertation.

2.1 Balance equations from continuum mechanics

Consider the generic body of Figure 7, which deforms according to a linear elastic regime of small displacements and deformations, subject to forces and displacements prescribed in parts of the boundary.

Figure 7 - Illustration of a generic elastic body subject to prescribed forces and displacements.

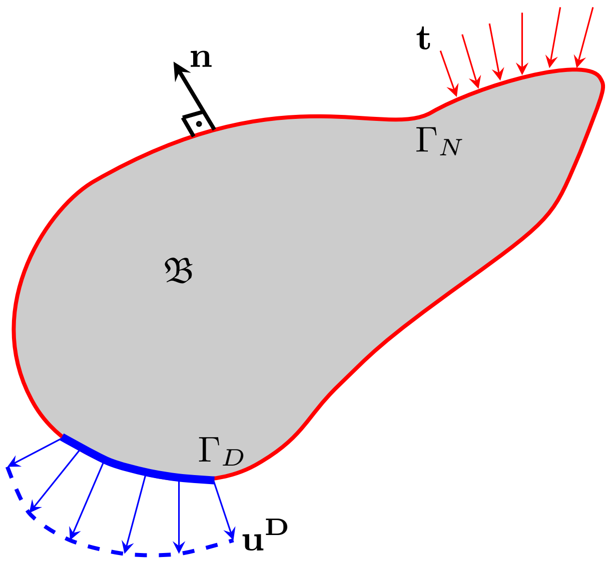

Let $\boldsymbol{\sigma}$ be the tensor stress, $\boldsymbol{u}$ the displacement field, $\boldsymbol{\epsilon}$ the tensor strain and $\boldsymbol{\mathcal{C}}$ the 4th order elasticity tensor, for this elastic solid. The boundary value problem of linear elasticity is defined by the following equations

$$
\begin{aligned}
\nabla \cdot \boldsymbol{\sigma}(\boldsymbol{u}) &= \mathbf{0} \;, && (1)\\
\boldsymbol{\sigma}(\boldsymbol{u}) &= \boldsymbol{\sigma}(\boldsymbol{u})^T \;, && (2)\\
\boldsymbol{\epsilon}(\boldsymbol{u}) &= \frac{1}{2}\left(\nabla \boldsymbol{u} \;+\; \nabla \boldsymbol{u}^T\right) \;, && (3)\\
\boldsymbol{\sigma}(\boldsymbol{u}) &= \boldsymbol{\mathcal{C}} : \boldsymbol{\epsilon}(\boldsymbol{u}) \;, && (4)
\end{aligned}
$$

with the following boundary conditions

$$
\begin{aligned}
\boldsymbol{\sigma}(\boldsymbol{u}) \cdot \boldsymbol{n} = \boldsymbol{t} \; in \; \Gamma_N \;, && (5)\\
\boldsymbol{u} = \boldsymbol{u^D} \; in \; \Gamma_D \;, && (6)
\end{aligned}
$$

where the Eq.(1) represents the balance of linear *momentum*, Eq.(2) is from the balance of angular *momentum*, Eq.(3) is a linear kinematic relationship between strain tensor and displacement field, and Eq.(4) represents a linear constitutive relationship between stress and strain tensors.. In the boundary conditions, Γ_D is the partition of $\partial\mathfrak{B}$ on which the displacements are prescribed, Γ_N is the complementary partition of $\partial\mathfrak{B}$ on which forces $\boldsymbol{t}$ are prescribed such that $\Gamma_D \cup \Gamma_N = \mathfrak{B}$ and $\Gamma_D \cap \Gamma_N = \emptyset$. This constitutive model is for small deformations of the linear elastic material and is the general Hooke Law (HJELMSTAD, 2005; SLAUGHTER, 2002).

2.2 Discretization of balance equations

After multiplying the Eq.(1) by a weight function $\boldsymbol{w}$ and integrating in all body volume $\mathfrak{B}$, one has the integral equation

$$\int_{\mathfrak{B}} \big(\nabla \cdot \boldsymbol{\sigma}(\boldsymbol{u})\big) \cdot \boldsymbol{w} \; dV = 0 \;, \tag{7}$$

where dV is a volume element of body $\mathfrak{B}$. Using integration by parts,

$$\int_{\mathfrak{B}} \big(\nabla \cdot \boldsymbol{\sigma}(\boldsymbol{u})\big) \cdot \boldsymbol{w} \; dV = \int_{\partial\mathfrak{B}} \big(\boldsymbol{\sigma}(\boldsymbol{u}) \cdot \boldsymbol{n}\big) \cdot \boldsymbol{w} \; dS - \int_{\mathfrak{B}} \boldsymbol{\sigma}(\boldsymbol{u}) : \nabla \boldsymbol{w} \; dV \;, \tag{8}$$

where dS is an area element in the surface $\mathfrak{B}$. Thus, recalling that $\boldsymbol{\sigma}(\boldsymbol{u}) \cdot \boldsymbol{n} = \boldsymbol{t}$ in Γ_N,

$$\int_{\Gamma_N} \boldsymbol{t} \cdot \boldsymbol{w} \; dS - \int_{\mathfrak{B}} \boldsymbol{\sigma}(\boldsymbol{u}) : \nabla \boldsymbol{w} \; dV = 0 \;, \tag{9}$$

and considering the Eq.(3), the Eq.(4) and $\nabla \boldsymbol{w} = \nabla \boldsymbol{w}^T$, the weak formulation of an elastic solid is expressed as

$$\int_{\mathfrak{B}} \boldsymbol{\epsilon}(\boldsymbol{u}) : \boldsymbol{\mathcal{C}} : \boldsymbol{\epsilon}(\boldsymbol{w}) \; dV = \int_{\Gamma_N} \boldsymbol{t} \cdot \boldsymbol{w} \; dS \; . \tag{10}$$

To discretize, the Galerkin method is used. The unknown and virtual fields (ZOHDI, 2018) are

$$\boldsymbol{u}(\boldsymbol{x}) \;=\; \boldsymbol{u}^D(\boldsymbol{x}) + \sum_{i=1}^{N} \boldsymbol{U}_i \boldsymbol{\Phi}^i(\boldsymbol{x}) \; , \tag{11}$$

$$\boldsymbol{w}(\boldsymbol{x}) \;=\; \sum_{j=1}^{N} \boldsymbol{U}_j \boldsymbol{\Phi}^j(\boldsymbol{x}) \; . \tag{12}$$

In this way, one obtains the expression

$$\sum_{j=1}^{N} \left[\int_{\mathfrak{B}} \boldsymbol{\epsilon}(\boldsymbol{u}^D) : \boldsymbol{\mathcal{C}} : \boldsymbol{\epsilon}(\boldsymbol{\Phi}^j) \; dV \right] \cancel{\boldsymbol{U}_j} \; + \; \sum_{j=1}^{N} \sum_{i=1}^{N} \left[\int_{\mathfrak{B}} \boldsymbol{\epsilon}(\boldsymbol{\Phi}^i) : \boldsymbol{\mathcal{C}} : \boldsymbol{\epsilon}(\boldsymbol{\Phi}^j) \; dV \right] \boldsymbol{U}_i \cancel{\boldsymbol{U}_j}$$
$$= \sum_{j=1}^{N} \left[\int_{\Gamma_N} \boldsymbol{t} \cdot \Phi^j dS \right] \cancel{\boldsymbol{U}_j} \; ,$$

$$\underbrace{\sum_{i=1}^{N} \sum_{j=1}^{N} \left[\int_{\mathfrak{B}} \boldsymbol{\epsilon}(\boldsymbol{\Phi}^i) : \boldsymbol{\mathcal{C}} : \boldsymbol{\epsilon}(\boldsymbol{\Phi}^j) \; dV \right]}_{[\mathbf{K}]} \underbrace{\boldsymbol{U}_i}_{\boldsymbol{U}} = \underbrace{\sum_{j=1}^{N} \left[\int_{\Gamma_N} \boldsymbol{t} \cdot \Phi^j dS \; - \; \int_{\mathfrak{B}} \boldsymbol{\epsilon}(\boldsymbol{u}^D) : \boldsymbol{\mathcal{C}} : \boldsymbol{\epsilon}(\boldsymbol{\Phi}^j) \; dV \right]}_{\mathbf{F_r}} ,$$

$$[\mathbf{K}]\mathbf{U} = \mathbf{F_r} \; , \tag{13}$$

being $[\mathbf{K}]$ stiffness matrix, $\mathbf{U}$ displacement vector and $\mathbf{F_r}$ force vector.

2.3 Criteria for structural integrity

This section presents the criteria for structural integrity that are used as structural optimization constraints.

2.3.1 The von Mises yield criterion

The stress state (stress vector), associated to direction $\boldsymbol{n}$ is calculated through the matrix vector by product between the stress tensor and $\boldsymbol{n}$, i.e., in matrix form, (SPENCER, 2004; IRGENS, 2008)

$$\begin{Bmatrix} t_x^{(n)} \\ t_y^{(n)} \\ t_z^{(n)} \end{Bmatrix} = \begin{bmatrix} \sigma_{xx} & \sigma_{xy} & \sigma_{xz} \\ \sigma_{yx} & \sigma_{yy} & \sigma_{yz} \\ \sigma_{zx} & \sigma_{zy} & \sigma_{zz} \end{bmatrix} \begin{Bmatrix} n_x \\ n_y \\ n_z \end{Bmatrix} , \tag{14}$$

or, in a simpler notation

$$\boldsymbol{t}^{(n)} = [\boldsymbol{\sigma}] \cdot \boldsymbol{n} . \tag{15}$$

In a state of stress at one point, the principal planes are those planes where the shear stress (tangential component) is zero. To determine the planes defined by the normal vectors $\boldsymbol{n}$, such that the stress vectors are acting only on them, consider

$$\boldsymbol{t}^{(n)} = \lambda\, \boldsymbol{n} . \tag{16}$$

Substituting in Eq.(15),

$$[\boldsymbol{\sigma}] \cdot \boldsymbol{n} = \lambda\, \boldsymbol{n} , \tag{17}$$

$$[\boldsymbol{\sigma}] \cdot \boldsymbol{n} - \lambda\, [\boldsymbol{I}]\, \boldsymbol{n} = \boldsymbol{0} , \tag{18}$$

$$\big([\boldsymbol{\sigma}] - \lambda[\boldsymbol{I}]\big) \cdot \boldsymbol{n} = \boldsymbol{0} , \tag{19}$$

being $[\boldsymbol{I}]$ the identity matrix. Therefore, the determination of the principal planes is reduced to the solution of an eigenvalue problem, where the eigenvector of the stress tensor defines the planes (principal directions) and the eigenvalues of the stress tensor, λ, are the principal stress. In possession of the principal stresses σ_1, σ_2 and σ_3, the criteria of structural integrity can be evaluated.

Consider a point at a state of triaxial stress. The deformation begins when the quadratic mean of the differences between the states of principal stresses is equal to that verified from the beginning of the deformation (JONES, 2009). Being S_Y the yield stress, the von Mises stress can be calculated by the expression

$$\sigma_{VM} = \sqrt{\frac{1}{2}\left[(\sigma_1 - \sigma_2)^2 + (\sigma_1 - \sigma_3)^2 + (\sigma_2 - \sigma_3)^2\right]} , \tag{20}$$

and according to von Mises criterion, the material behaves elastically when

$$\sigma_{VM} \leq S_Y . \tag{21}$$

2.3.2 Buckling

For bars, buckling is a phenomenon that occurs in slender structural parts (the cross-sectional area is small in relation to its length) when an axial compression effort is present. It happens when the structural part undergoes transverse bending when submitted to an axial compression ($\sigma < 0$), causing a stability loss. The critical buckling load is also known as the Euler load critical (JONES, 2009). Considering each structural element as a bar hinged at the ends, the following formula defines the stress referring to buckling:

$$\sigma^E = \frac{\pi^2 \; E \; I}{L^2 \; A} \;, \tag{22}$$

where E is Young's modulus, I is moment of inertia, L is the length and A is the cross area. Let σ^c be the compression stress ($\sigma < 0$) and σ^t be the tensile stress ($\sigma > 0$). Under von Mises criterion (equivalent stress), to avoid buckling,

$$\sigma^c \leq \sigma^E \; . \tag{23}$$

The general criterion of structural integrity, for bars that are subjected to compressive stresses, takes into account yield and buckling, considering the system as safe if

$$\sigma^c \leq \min \left(\sigma^E \; , \; S_Y \right) . \tag{24}$$

2.4 **Structural optimization**

The objective of the structural optimization problem treated in this dissertation is the reduction of the mass while respecting the criteria of structural integrity. The density, denoted by ρ is a scalar field that represents a local ratio between mass and volume (IRGENS, 2008). The mass of an elastic body $\mathfrak{B}$, in the generic form, is given by,

$$m(x) \;=\; \int_{\mathfrak{B}} \rho(x) \; dV \tag{25}$$

The objective function of the structural optimization problem is the minimization of the Eq.(25), i.e., mass minimization.

The constraints of the structural optimization problem, which are in Eq.(24), are evaluated using the balance equations: solving a system of partial differential equations with the Eq.(1), Eq.(2), Eq.(3) and Eq.(4), under boundary conditions Eq.(5) and Eq.(6). After calculating the Von Mises criterion and buckling, one has the constraints.

2.5 Finite element analysis

In order to gain some insight into the truss behavior, a finite element analysis (FEA) is done before the structural optimization process. The structural models analyzed in this dissertation are trusses. The equilibrium equations are obtained from the principle of virtual work, being written as the following matrix system shown in section 3.2,

$$[\mathbf{K}]\,\mathbf{U} = \mathbf{F_r}\ , \tag{26}$$

where $[\mathbf{K}]$ is the stiffness matrix, $\mathbf{U}$ is the displacement vector and $\mathbf{F_r}$ is force vector, which are respectively defined by

$$\mathbf{U} = \begin{bmatrix} u_1 & v_1 & u_2 & v_2 & u_3 & v_3 & u_4 & v_4 & \cdots & \cdots & u_n & v_n \end{bmatrix}^T\ , \tag{27}$$

and

$$\mathbf{F_r} = \begin{bmatrix} f_{r1} & f_{r2} & f_{r3} & f_{r4} & f_{r5} & f_{r6} & f_{r7} & f_{r8} & f_{r9} & \cdots & \cdots & f_{rD} \end{bmatrix}^T\ . \tag{28}$$

The number of nodes is n and D is number of degrees of freedom. The stiffness matrix $[\mathbf{K}]$ is obtained by the expression

$$[\mathbf{K}] = \sum_{e=1}^{N} [\overline{\mathbf{K}}_e]\ , \tag{29}$$

where N is the number of elements and $[\overline{\mathbf{K}}_e]$ is the elementary stiffness matrix. In global coordinates the elementary stiffness matrix of the bar e is given by

$$[\overline{\mathbf{K}}_e] = \frac{A_e E}{L_e} \begin{bmatrix} \cos^2\theta_e & \cos\theta_e\sin\theta_e & -\cos^2\theta_e & -\cos\theta_e\sin\theta_e \\ \cos\theta_e\sin\theta_e & \sin^2\theta_e & -\cos\theta_e\sin\theta_e & -\sin^2\theta_e \\ -\cos^2\theta_e & -\cos\theta_e\sin\theta_e & \cos^2\theta_e & \cos\theta_e\sin\theta_e \\ -\cos\theta_e\sin\theta_e & -\sin^2\theta_e & \cos\theta_e\sin\theta_e & \sin^2\theta_e \end{bmatrix}, \tag{30}$$

where A_e is the cross-sectional area, E is the material modulus of elasticity, L_e is the element length and θ_e is the angle formed between the bar longitudinal axis and the horizontal axis of the reference system (x axis) (FERREIRA, 2009).

The local mass matrix of the finite elements for the linear 2D truss element can be calculated as

$$[\mathbf{M_e}] = \frac{\rho A_e L_e}{6}\begin{bmatrix} 2 & 0 & 1 & 0 \\ 0 & 2 & 0 & 1 \\ 1 & 0 & 2 & 0 \\ 0 & 1 & 0 & 2 \end{bmatrix} . \tag{31}$$

The mass matrix $[\mathbf{M}]$ is obtained by expression

$$[\mathbf{M}] = \sum_{e=1}^{N} [\overline{\mathbf{M}}_e] . \tag{32}$$

where $[\overline{\mathbf{M}}_e]$ is the elementary mass matrix in global coordinates.

The natural frequencies of a structural model are obtained by the following eigenvalue problem,

$$[\mathbf{K}]\boldsymbol{\phi} = \omega^2[\mathbf{M}]\boldsymbol{\phi} , \tag{33}$$

being ω^2 the eigenvalue and $\boldsymbol{\phi}$ the eigenvector, where ω is the value of the natural frequency. This work uses the `Matlab` function "eig" to obtain these values. The natural frequencies obtained by Eq.(33) are in rad/s. To obtain the natural frequencies in Hz, simply divide the values of ω by 2π.

There is a standardization in the mathematical formulation as of the second model where the mass, stress, and constraints are calculated in the same way in these structural models. The total mass of the two-dimensional truss is

$$m = \sum_{e=1}^{N} m_e = \sum_{e=1}^{N} \rho \, L_e \, A_e . \tag{34}$$

The normal stress at the bar e is obtained by expression

$$\sigma_e = E \, \mathbf{B}_e \, \mathbf{U}_e , \tag{35}$$

where

$$\mathbf{B}_e = \frac{1}{L_e}\left[\, -\cos\theta_e \quad -\sin\theta_e \quad \cos\theta_e \quad \sin\theta_e \, \right] , \tag{36}$$

being $\mathbf{B}_e$ the deformation matrix and $\mathbf{U}_e$ the displacement in bar e.

The four structural integrity criteria employed in this dissertation are defined by following their respective structural properties, respectively: yield stress, buckling, natural frequencies, and displacements.

The integrity criterion related to yield stress can be written as

$$\frac{|\sigma_e|}{S_y} - 1 \leq 0, \qquad e = 1, \cdots, N \ . \tag{37}$$

The buckling criterion is considered only when the stress is compressive, i.e., $\sigma_e < 0$. A buckling constraint is defined by

$$\frac{-\ \sigma_e}{\sigma_e^E} - 1 \leq 0, \qquad e = 1, \cdots, N \ . \tag{38}$$

Considering a structural optimization problem having as constraints three natural frequencies, w_1^*, w_2^* and w_3^*, one has the expression for the constraints related to natural frequencies,

$$1 - \frac{\omega_1}{w_1^*} \leq 0 \ , \tag{39}$$

$$1 - \frac{\omega_2}{w_2^*} \leq 0 \ , \tag{40}$$

$$1 - \frac{\omega_3}{w_3^*} \leq 0 \ . \tag{41}$$

Defining a maximum displacement $d_{p_{max}}$ for the nodes of the structural model and considering this a constraint for a structural optimization problem, the constraints related to maximum displacement are obtained by the expression,

$$\frac{d_{p_n}}{d_{p_{max}}} - 1 \leq 0 \ , \tag{42}$$

remembering that n is the node number. The d_{p_n} is the displacement in each node n, and with the values of the $\boldsymbol{U}$,

$$d_{p_n} = \sqrt{u_n^2 + v_n^2} \ . \tag{43}$$

The structural optimization problem considered here aims to minimize the structure mass, Eq.(34), using d_i and t as design variables, considering as constraints the inequalities in Eq.(37), and a limited set of values for d and t, i.e.,

$$d_{imin} \leq d_i \leq d_{imax} \qquad \text{and} \qquad t_{min} \leq t \leq t_{max}. \tag{44}$$

In the cases which present variation of the cross-section areas and of height (shape optimization),

$$A_{emin} \leq A_e \leq A_{emax} \qquad \text{and} \qquad H_{min} \leq H \leq H_{max} \ . \tag{45}$$

3 NUMERICAL METHODS

In this chapter, aiming to simplify the presentation of numerical methods for optimization, a generic formulation of an optimization problem is made, followed by addressing specifically three optimization methods, SQP, GA and CE. From the generic formulation, the three methods are addressed, following the same nomenclature of the generic formulation. At the end of the chapter, a simple objective function is used for comparison between the three methods.

3.1 Generic formulation of an optimization problem

Let $\mathbb{R}^n$ be the n-dimensional Euclidean space, $\boldsymbol{x}$ the vector with the problem variables, $\mathcal{J}$ the objective function, p_i and q_i problem constraints; where $\mathcal{J} : \mathbb{R}^n \to \mathbb{R}$, $p_i : \mathbb{R}^n \to \mathbb{R}$ and $q_j : \mathbb{R}^n \to \mathbb{R}$. An abstract (generic) optimization problem can be formulated as follows,

$$\boxed{\begin{array}{l} \text{Find } \boldsymbol{x} \in \mathbb{R}^n \text{ that maximize,} \\ \qquad \mathcal{J}(\boldsymbol{x}) \quad , \\ \text{subject to the restrictions} \\ \qquad p_i(\boldsymbol{x}) = 0 \quad i = 1, 2, \ldots, M \quad , \\ \qquad q_j(\boldsymbol{x}) \leq 0 \quad j = 1, 2, \ldots, N \quad . \end{array}} \tag{46}$$

In an optimization problem, one defines a “range” to find the optimal value of the variable. Therefore, one defines x_{min} and x_{max}, where $x_{min} \leq x \leq x_{max}$. This inequality is valid for each component of vector $\boldsymbol{x}$. In structural optimization the main objective is the reduction of the mass while respecting the structural criteria. For this reason, there is a minimization in the generic formulation. In the structural integrity criteria, one has values that are the constraints of the structural optimization, and in the cases addressed only the restriction $q_j \leq 0$ is used.

The generic formulation of an optimization problem can be presented more elegantly as,

$$\boxed{\begin{array}{l} \text{Find } \boldsymbol{x}^\star = \arg \max\limits_{\boldsymbol{x} \in \mathcal{A}_{adm}} \mathcal{J}(\boldsymbol{x}) \ , \\ \text{where} \\ \mathcal{A}_{adm} = \{\boldsymbol{x} \in \mathbb{R}^n \ , \ p_i(\boldsymbol{x}) = 0 \ , \ i = 1, 2, \ldots, M \text{ and} \\ \qquad\qquad\qquad q_j(\boldsymbol{x}) \leq 0 \ , \ j = 1, 2, \ldots, N\} \ . \end{array}} \tag{47}$$

If the optimization problem is minimization instead of maximization, consider a "dual relation" and add a negative sign in $\mathcal{J}$,

$$\min \mathcal{J}(\boldsymbol{x}) = \max(-\mathcal{J}(\boldsymbol{x})) \ . \tag{48}$$

3.2 **Sequential quadratic programming**

Sequential quadratic programming (SQP) transforms the constrained optimization problem into an unconstrained problem and constructs a sequence of approximations, approximating the objective function for a quadratic function and the constraints for linear functions, via Lagrange multipliers (BONNANS et al., 2009). For optimization problems of minimization, the Lagrangian is,

$$\mathcal{L}(\boldsymbol{x}, \boldsymbol{\lambda}_p, \boldsymbol{\lambda}_q) = \mathcal{J}(\boldsymbol{x}) - \boldsymbol{\lambda}_p^T p_i(\boldsymbol{x}) - \boldsymbol{\lambda}_q^T q_j(\boldsymbol{x}) \ , \tag{49}$$

where $\boldsymbol{\lambda}_p$ and $\boldsymbol{\lambda}_q$ are vectors of Lagrange multipliers. Considering an iteration $\boldsymbol{x}^k$, the SQP starts a search direction $\boldsymbol{d}$ as a solution to the subproblem with the approximations,

$$\mathcal{L}(\boldsymbol{x}, \boldsymbol{\lambda}_p, \boldsymbol{\lambda}_q) \approx \mathcal{L}(\boldsymbol{x}^k, \boldsymbol{\lambda}_p^k, \boldsymbol{\lambda}_q^k) + \nabla \mathcal{L}(\boldsymbol{x}^k, \boldsymbol{\lambda}_p^k, \boldsymbol{\lambda}_q^k) \ \boldsymbol{d} + \frac{1}{2} \boldsymbol{d}^T \mathcal{H}_{ij}[\mathcal{L}(\boldsymbol{x}, \boldsymbol{\lambda}_p, \boldsymbol{\lambda}_q)] \ \boldsymbol{d} \ , \tag{50}$$

$$p_i(\boldsymbol{x}) \approx p(\boldsymbol{x}^k) + \nabla p(\boldsymbol{x}^k) \ \boldsymbol{d} \ , \tag{51}$$

$$q_j(\boldsymbol{x}) \approx q(\boldsymbol{x}^k) + \nabla q(\boldsymbol{x}^k) \ \boldsymbol{d} \ , \tag{52}$$

where

$$\boldsymbol{d} = \boldsymbol{x} - \boldsymbol{x}^k \ , \tag{53}$$

$$\mathcal{H}_{ij} = \frac{\partial^2}{\partial x_i^k \partial x_j^k} \ . \tag{54}$$

where $\mathcal{H}$ is a differential operator. $\mathcal{H}_{ij}[\mathcal{L}(\boldsymbol{x}, \boldsymbol{\lambda}_p, \boldsymbol{\lambda}_q)]$ is a Hessian.

For optimization problems of minimization, SQP constructs a sequence of approximations for $\boldsymbol{x}^\star$, denoted $\boldsymbol{x}_{k+1} = \boldsymbol{d}_k + \boldsymbol{x}_k$ where each iteration solves subproblems of the form:

$$\boxed{\begin{array}{l} \text{Find } \boldsymbol{d} \in \mathbb{R}^n \text{ such that} \\ \qquad \min \nabla \mathcal{L}(\boldsymbol{x}^k, \boldsymbol{\lambda}_p^k, \boldsymbol{\lambda}_q^k)^T \ \boldsymbol{d} + \frac{1}{2}\boldsymbol{d}^T \boldsymbol{B}^k \boldsymbol{d} \quad , \\ \\ \text{where } \boldsymbol{B}^k = \mathcal{H}_{ij}\mathcal{L}(\boldsymbol{x}^k, \boldsymbol{\lambda}_p^k, \boldsymbol{\lambda}_q^k) \quad , \\ \\ \text{such that} \\ \quad p_i(\boldsymbol{x}^k) + \nabla p_i(\boldsymbol{x}^k)^T \ \boldsymbol{d} = 0 \ , \ i = 1, 2, \ldots, M \quad , \\ \quad q_i(\boldsymbol{x}^k) + \nabla q_j(\boldsymbol{x}^k)^T \ \boldsymbol{d} \leq 0 \ , \ j = 1, 2, \ldots, N \quad . \end{array}} \tag{55}$$

The SQP is a first-order method when the gradient of the objective function and of the constraints is provided. When the Hessian is also provided, SQP is a second-order method. If the Hessian is not provided, an approximation is found by the BFGS method, cited in section 1.3.2.

3.3 Genetic algorithm

Genetic algorithm (GA) is an optimization method based on the biological concept of natural evolution. The GA maintains a population of solutions, which can be called individuals, and modifies these groups using different operators until achieving the desired improvement. The GA is formed by three specific steps: selection, crossover and mutation.

This algorithm originates from the work of Holland and his collaborators (HOLLAND, 1992) and has a philosophical basis in Darwin's theory of the survival of those that are most adapted to the environment (DARWIN, 2009). In a way analogous to the natural process where a population of a given species adapts to its natural habitat, a population of projects (candidates for solving the optimization problem) is then created, allowing it to adapt to the project space.
In the natural process, by analogy, genetic information is stored in chains of chromosomes that are altered through generations for adaptation of the environment. This chromosomal structure represents generation memory and is altered by the reproduction of individuals. In addition to reproduction, occasional mutations of genetic information may alter the constitution of the chromosomes (SILVA NETO; BECCENERI, 2009).

The more adapted members of the population will be more likely to be selected, contributing more to the improvement in the constitution of the chromosomes. This process is facilitated if a fitness function ($\mathcal{J}_{fit}$) is defined, which will be a measure of how good the individual is in relation to the others in a given generation in the process of evolution. For problems without constraints, $\mathcal{J}_{fit}$ will serve as its own objective function. For a problem with constraints, the penalty can be used to transform into an unconstrained problem.

The following objective function is used as an example,

$$\mathcal{J}(x) = e^{-(x-2)^2} + 0.8e^{-(x+2)^2} \tag{56}$$

In this case, since it regards maximization and because it has no constraints, one can use $\mathcal{J}_{adap} = \max \mathcal{J}(x)$. Therefore the fitness function is

$$\mathcal{J}_{fit} = e^{-(x-2)^2} + 0.8e^{-(x+2)^2} \tag{57}$$

The variable will be converted to its binary equivalent, being mapped to a fixed-length string of 0 and 1. The numerical precision of each variable (solution) will determine the length of this string. If we consider a chain of 10 binary digits, the minimum and maximum values will be

$$(X_i)_{min} = 0000000000 \ ,$$
$$(X_i)_{max} = 1111111111 \ .$$

A linear mapping would convert intermediate values of real numbers and values as follows,

$$\mathbb{X} = X^{(l)} + \frac{X^{(u)} - X^{(l)}}{2^{\varphi} - 1} X_{bin} \ , \tag{58}$$

where $X^{(u)}$ is the maximum real value, $X^{(l)}$ is the minimum real value, φ is the length of the binary chain and X_{bin} is the value corresponding to the current binary, which can be calculated as

$$X_{bin} = \sum_{K=0}^{\varphi-1} 2^k b_k \tag{59}$$

where $b_k = 0$ or 1. Because they have only one variable, a 10-digit string represents the solution to this problem. If 4 variables were considered, four binary numbers corresponding to each variable are juxtaposed, forming a chain of 40 digits of 0 and 1, that is, 10 digits for each variable (SILVA NETO; BECCENERI, 2009).

3.3.1 Selection

The selection process is biased towards producing better adapted members and eliminating less well-adapted members. Among several existing ways, the simplest to select the members of the crossover, is to assign a probability to each member based on their adaptability function. If ϖ_i is the measure of adaptability of the i-th member, this probability can be associated with this member $\varpi_i / \sum_{Ps} \varpi_i$, where Ps is the population size a new population of the same previous size is generated, but with a higher average of adaptability. A widely used idea is to elucidate the individual of the population that is well adapted (greater value of the adaptability function) directly to the next generation (SILVA NETO; BECCENERI, 2009).

3.3.2 Crossover

The crossover process allows the characteristics of several projects to be interchangeable, creating a more adapted generation. A common type of crossing can be done by selecting two parents, based on their respective odds of being chosen, randomly choosing one or two points in the (binary) genetic chain and changing the digits 1 and 0 between the two parents. In the literature, other types of crossing can be found (SILVA NETO; BECCENERI, 2009).

3.3.3 Mutation

The mutation protects the genetic search for a premature loss of good genetic material during screening and crossing. The mutation process is simply done by choosing a few members of the population and, accordingly, a probability of 0 is changed to 1 (and vice versa) at a randomly chosen point in its binary chains (SILVA NETO; BECCENERI, 2009).

A binary with φ digits allows the representation of 2^{φ} values of a continuous variable. If the continuous variable has an accuracy A_c, then the number of digits of the binary string will be estimated,

$$2^{\varphi} \geq \frac{(X^{(u)} - X^{(l)})}{A_c} + 1 \ , \tag{60}$$

where A_c represents the precision of the variables (resolution). When GA deals with discrete internal variables, $A_c = 1$, so GA performs well with the entire discrete variables (SILVA NETO; BECCENERI, 2009).

3.4 Cross-entropy method

The Cross-entropy method (CE) is a Monte Carlo technique used for estimation and optimization. In the estimation setting, the CE provides a form of searching for the sampling of optimal importance. After formulating an optimization problem as an estimation problem, CE becomes a powerful stochastic search method. The method is based on a simple iterative procedure and in each iteration it contains only two phases: generating the random data samples (trajectories, vectors, etc.) and updating the parameters of random mechanisms based on the data, in order to produce a better sample in the next iteration (KROESE; TAIMRE; BOTEV, 2011).

The CE has its origin in the adaptation of the algorithm to estimate a rare event based on variance minimization. This procedure was soon modified to an algorithm adapted for estimation of rare events and combinatorial optimization, where the minimum variation programs were replaced by the CE minimization program (BOTEV et al., 2013).

To explain how CE works for optimization, it is necessary to explain how it works for estimation and for rare-event probability estimation. Before starting with estimation, one needs to have some definitions.

An experiment that is repeated with the same conditions and produces different results is called a random experiment. A random experiment is described by a triplet, (Ω, Σ, $\mathcal{P}$), dubbed probability space, where Ω is the sample space (set of all possible events), Σ is the set of all relevant events and $\mathcal{P}$ is the measure of probability (a measure of the expectation of an event to occur).

A random variable is a mapping $X : \Omega \to \mathbb{R}$ defined on the probability space (Ω, Σ, $\mathcal{P}$) for which the preimage of every real number under X is a relevant event.

Let F be the probability distribution of X, also known as cumulative distribution function (CDF), defined as the probability of elementary event $\{X \leq x\}$, i.e.,

$$F(x) = \mathcal{P}\{X \leq x\} \ . \tag{61}$$

If the function F is differentiable,

$$f(x) = dF(x)/dx \ , \tag{62}$$

f is called the probability density function (PDF) of X, and one has

$$F(x) = \int_{-\infty}^{x} f(\xi) d\xi \ . \tag{63}$$

The expectation of a random variable X is

$$\mathbb{E}\{X\} = \int_{\mathbb{R}} x \; dF(x) \; . \tag{64}$$

The mean value of a random variable X is defined as

$$\begin{aligned} \mu &= \mathbb{E}\{X\} \; , \\ &= \int_{\mathbb{R}} x \; dF(x) \; , \\ &= \int_{\mathbb{R}} x \; f(x) \; dx \; . \end{aligned} \tag{65}$$

The variance of a random variable X is defined as

$$\begin{aligned} s^2 &= \mathbb{E}\{(X-\mu)^2\} \; , \\ &= \int_{\mathbb{R}} (x-\mu)^2 \; dF(x) \; , \\ &= \int_{\mathbb{R}} (x-\mu)^2 \; f(x) \; dx \; . \end{aligned} \tag{66}$$

The variance can also be written as

$$s^2 = \mathbb{E}\{X^2\} - \mu^2 \; . \tag{67}$$

Let $\boldsymbol{x} = (x_1, x_2, \ldots, x_n) \in \mathbb{R}^n$, where $\boldsymbol{x}$ is a vector with problem variables, then a random vector $\boldsymbol{X} = (X_1, X_2, \ldots, X_n)$ is a collection of n random variables that may be considered a (measurable) mapping $\boldsymbol{X} : \Omega \to \mathbb{R}^n$, where a collection of event in Ω is mapped into a region on the n-dimensional Euclidean space $\mathbb{R}^n$ under such mapping.

3.4.1 Importance sampling estimator

Considering $\mathbb{E}_f$ the expectation using the PDF designated by f, define ℓ as

$$\ell = \mathbb{E}_f\{\mathcal{J}(\boldsymbol{X})\} = \int_{\mathbb{R}^n} \mathcal{J}(\boldsymbol{x}) \; f(\boldsymbol{x}) \; d\boldsymbol{x} \; , \tag{68}$$

where $\mathcal{J}$ is the objective function, and f is the PDF of the continuous random vector $\boldsymbol{X}$. Let g be other PDF in which $g(\boldsymbol{x}) = 0$ implies that $\mathcal{J}(\boldsymbol{X}) \; f(\boldsymbol{X}) = 0$ for all $\boldsymbol{x}$ (KROESE; TAIMRE; BOTEV, 2011; RUBINSTEIN; KROESE, 2017). So one can rewrite,

$$\ell = \int_{\mathbb{R}^n} \mathcal{J}(\boldsymbol{x}) \; \frac{f(\boldsymbol{x})}{g(\boldsymbol{x})} \; g(\boldsymbol{x}) \; d\boldsymbol{x} = \mathbb{E}_g \left\{ \mathcal{J}(\boldsymbol{X}) \; \frac{f(\boldsymbol{X})}{g(\boldsymbol{X})} \right\} \; . \tag{69}$$

If $\boldsymbol{X}_1, \boldsymbol{X}_2, \ldots, \boldsymbol{X}_N$ are independently and identically distributed (*iid*) in g,

$$\hat{\ell} = \frac{1}{N} \sum_{K=1}^{N} \mathcal{J}(\boldsymbol{X}_k) \frac{f(\boldsymbol{X}_k)}{g(\boldsymbol{X}_k)} , \tag{70}$$

is an unbiased importance sampling estimator of ℓ.

3.4.2 Kullback-Leibler divergence

An alternative approach to the minimum variation method used in CE to choose an "optimal" sample distribution is based on the Kullback-Leibler divergence (RUBISTEIN; KROESE, 2004). This divergence between the two continuous PDFs g and h is given by

$$\begin{aligned} \mathcal{D}(g,h) = \mathbb{E}_g \left\{ \ln \frac{g(\boldsymbol{X})}{h(\boldsymbol{X})} \right\} &= \int_{\mathbb{R}^n} g(\boldsymbol{x}) \ln \frac{g(\boldsymbol{x})}{h(\boldsymbol{x})}\, d\boldsymbol{x} \\ &= \int_{\mathbb{R}^n} g(\boldsymbol{x}) \ln g(\boldsymbol{x})\, d\boldsymbol{x} - \int_{\mathbb{R}^n} g(\boldsymbol{x}) \ln h(\boldsymbol{x})\, d\boldsymbol{x} . \end{aligned} \tag{71}$$

Since the choice of the importance sampling density is crucially linked to the variance (Var) of the estimator $\hat{\ell}$, one considers the minimization of the variance of $\hat{\ell}$ with respect to g (RUBINSTEIN; KROESE, 2017),

$$\min_g Var_g \left(\mathcal{J}(\boldsymbol{X}) \frac{f(\boldsymbol{X})}{g(\boldsymbol{X})} \right) . \tag{72}$$

The solution of the problem (72) is (RUBINSTEIN; MELAMED, 1998)

$$g^\star = \frac{|\mathcal{J}(\boldsymbol{x})| f(\boldsymbol{x})}{\int_{\mathbb{R}^n} |\mathcal{J}(\boldsymbol{x})| f(\boldsymbol{x})\, d\boldsymbol{x}} , \tag{73}$$

where $g^\star$ is optimal importance sampling density. If $\mathcal{J}(\boldsymbol{x}) \geq 0$, then

$$g^\star = \frac{|\mathcal{J}(\boldsymbol{x})| f(\boldsymbol{x})}{\ell} . \tag{74}$$

The idea of CE is to choose a probability density of importance h such that the Kullback-Leibler divergence between the optimal probability density $g^\star$ and h is minimal. Let $h^\star$ be the solution of the functional optimization problem,

$$\min_{h^\star} \mathcal{D}\ (g^\star, h) . \tag{75}$$

The probability density h is parameterized by a finite-dimensional vector $\boldsymbol{u}$, denoting $f(\boldsymbol{x}) = f(\boldsymbol{x};\boldsymbol{u})$ and $h(\boldsymbol{x}) = f(\boldsymbol{x};\boldsymbol{v})$, where $\boldsymbol{v}$ is a reference parameter and the intention is to find the optimum of these parameters. One can say that $\min_{h^\star} \mathcal{D}\left(g^\star, h\right)$ is equal to

$$\max \int_{\mathbb{R}^n} g^\star(\boldsymbol{x}) \ln f(\boldsymbol{x};\boldsymbol{v})\ d\boldsymbol{x}\ , \tag{76}$$

as

$$g^\star = \frac{|\mathcal{J}(\boldsymbol{x})| f(\boldsymbol{x};\boldsymbol{u})}{\ell}\ , \tag{77}$$

and $\boldsymbol{v}$ is the reference parameter that needs to be found and has terms that do not depend on it. Minimizing Kullback-Leibler divergence between $g^\star$ and $f(\cdot;\boldsymbol{v})$ is equivalent to maximizing with respect to $\boldsymbol{v}$,

$$\boldsymbol{v}^\star = \operatorname*{argmax}_{\boldsymbol{v}} \int_{\mathbb{R}^n} \mathcal{J}(\boldsymbol{x}) f(\boldsymbol{x};\boldsymbol{u})\ \ln f(\boldsymbol{x};\boldsymbol{v})\ d\boldsymbol{x}\ . \tag{78}$$

If $\mathbb{E}_u\{\mathcal{J}(\boldsymbol{X})\} = \int \mathcal{J}(\boldsymbol{x}) f(\boldsymbol{x};\boldsymbol{u})\ d\boldsymbol{x}$,

$$\begin{aligned} \int_{\mathbb{R}^n} \mathcal{J}(\boldsymbol{x}) f(\boldsymbol{x};\boldsymbol{u}) d\boldsymbol{x} &= \int_{\mathbb{R}^n} \mathcal{J}(\boldsymbol{x}) \frac{f(\boldsymbol{x};\boldsymbol{u})}{f(\boldsymbol{x};\boldsymbol{w})} f(\boldsymbol{x};\boldsymbol{w})\ d\boldsymbol{x} \\ &= \mathbb{E}_w \left\{ \mathcal{J}(\boldsymbol{X}) \frac{f(\boldsymbol{x};\boldsymbol{u})}{f(\boldsymbol{x};\boldsymbol{w})} \right\}\ . \end{aligned} \tag{79}$$

Defining the likelihood ratio $W(\boldsymbol{x};\boldsymbol{u},\boldsymbol{w}) = f(\boldsymbol{x};\boldsymbol{u})/f(\boldsymbol{x};\boldsymbol{w})$, one has

$$\boldsymbol{v}^\star = \max_{\boldsymbol{v}}\ \mathbb{E}_w\{\mathcal{J}(\boldsymbol{X}) W(\boldsymbol{x};\boldsymbol{u},\boldsymbol{w})\}\ . \tag{80}$$

Using the Eq.(69) and Eq.(70) and then substituting in Eq.(80),

$$\boldsymbol{v}^\star = \max_{\boldsymbol{v}} \frac{1}{N} \sum_{k=1}^{N} \mathcal{J}(\boldsymbol{X}_k) W(\boldsymbol{X}_k;\boldsymbol{u},\boldsymbol{w}) \ln f(\boldsymbol{X}_k;\boldsymbol{v}), \tag{81}$$

where $W(\boldsymbol{X}_k;\boldsymbol{u},\boldsymbol{w}) = f(\boldsymbol{x}_k;\boldsymbol{u})/f(\boldsymbol{x}_k;\boldsymbol{w})$ is the likelihood ratio.

3.4.3 Rare-event probability estimation

Let $\mathcal{J}(\boldsymbol{X})$ again be denoted as the performance of the sample, where $\boldsymbol{X} \sim f(\cdot;\boldsymbol{u})$, and it is desired to estimate $\ell = \mathcal{P}_u(\mathcal{J}(\boldsymbol{X} \geq \gamma) = \mathbb{E}_u\{\mathbb{1}_{\{\mathcal{J}(\boldsymbol{X}) \geq \gamma\}}\}$, for a fixed level γ. Note that the estimation problem presents a particular case of ℓ with $\mathcal{J}(\boldsymbol{X}) = \mathbb{1}_{\{\mathcal{J}(\boldsymbol{X}) \geq \gamma\}}$. One assumes as before that $\boldsymbol{X}$ has a PDF $f(\cdot;\boldsymbol{u})$ in some family $f(\cdot;\boldsymbol{v})$. Thus, one has the estimator $\hat{\ell}$,

$$\hat{\ell} = \frac{1}{N}\sum_{K=1}^{N} \mathbb{1}_{\{\mathcal{J}(\boldsymbol{X}_k)\geq\gamma\}} \frac{f(\boldsymbol{X}_k;\boldsymbol{u})}{g(\boldsymbol{X}_k)} \ . \tag{82}$$

The Figure 8 shows a generalized distribution presenting an estimation of rare event, with indication of γ.

Figure 8 - Generic distribution with indication γ.

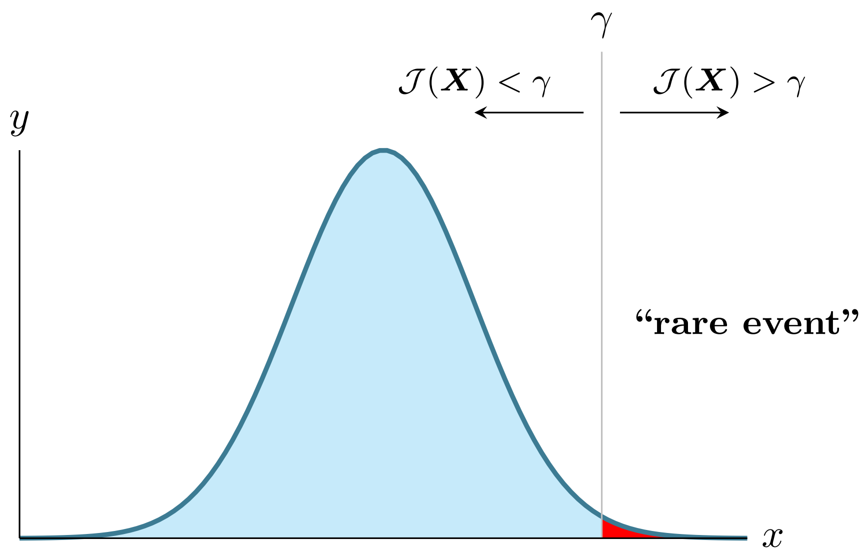

If $\mathcal{J}(x) = \mathbb{1}_{\{\mathcal{J}(\boldsymbol{X})\geq\gamma\}}$, so

$$\mathcal{J}(X_k) = 1 \ , \ if \ \mathcal{J}(\boldsymbol{X}) \geq \gamma \ ,$$
$$\mathcal{J}(X_k) = 0 \ , \ if \ \mathcal{J}(\boldsymbol{X}) < \gamma \ .$$

As you are considering an rare-event estimation, one has

$$\boldsymbol{v}^{\star} = \max_{\boldsymbol{v}} \frac{1}{N}\sum_{X_k \epsilon \mathcal{E}}^{N} W(\boldsymbol{X}_k;\boldsymbol{u},\boldsymbol{v}) \ln f(\boldsymbol{X}_k;\boldsymbol{v}), \tag{83}$$

where $\mathcal{E}$ are elite samples; $\boldsymbol{X}_k$ are values for which $\mathcal{J}(\boldsymbol{X}_k) \geq \gamma$. Normally ℓ is considered a rare event in the literature when it is less than 10^{-4}.

3.4.4 Cross-entropy algorithm for rare-event estimation

In cases where the CE is used in multilevel, where the reference parameters are considered as $\hat{\boldsymbol{v}}_{ti}$ and the levels as $\hat{\gamma}_{ti}$, the algorithm is constructed with the aim of promoting convergence for $\boldsymbol{v}^\star$ and $\gamma^\star$ (last level). In each iteration ti, one simulates N independent random variables $\boldsymbol{X}_1, \ldots, \boldsymbol{X}_N$ of the current density of the estimated importance sample, $f(\cdot; \hat{\boldsymbol{v}}_{ti-1})$, and sets $\hat{\gamma}_{ti}$ to be $(1-\varrho)$, which is the quantile of performance values $\mathcal{J}_{(\boldsymbol{X}_1)}, \ldots, \mathcal{J}_{(\boldsymbol{X}_N)}$, with $\hat{\gamma}_{ti} = \mathcal{J}_{(N^s - N^e + 1)}$, where ϱ is a specified primary parameter called a rarity parameter. Then one updates the value of $\hat{\boldsymbol{v}}_{ti-1}$ to $\hat{\boldsymbol{v}}_{ti}$, where $\hat{\boldsymbol{v}}_{ti}$ is calculated using the maximization of probability equivalent to the minimization of Kullback-Leibler divergence based on $N^e = [\varrho N^s]$ random variables, so that $\mathcal{J}(\boldsymbol{X}_i) \geq \hat{\gamma}_{ti}$.

Given the sample size N^s and the ϱ parameter, perform the following steps, in according with (BOTEV et al., 2013),

CE Algorithm for Rare-Event Estimation
1. Define $\boldsymbol{v}_0 = \boldsymbol{v}$. Let $N^e = [\varrho N^s]$. Set $ti = 1$.(iteration counter) ;
2. Generate $\boldsymbol{X}_1, \ldots, \boldsymbol{X}_N \sim$ identically distributed ($\sim iid$). Calculate $\mathcal{J}_i = \mathcal{J}(\boldsymbol{X}_i)$ for all i, and order these from smallest to largest: $\mathcal{J}_{(1)} \leq \ldots \leq \mathcal{J}_{(N)}$. Let $\hat{\gamma}_{ti}$ be the sample $(1-\varrho)$ - quantile of performances; that is, $\hat{\gamma}_{ti} = \mathcal{J}_{(N^s - N^e + 1)}$. If $\hat{\gamma}_{ti} > \gamma$, reset, $\hat{\gamma}_{ti}$ to γ ;
3. Use the same sample $\boldsymbol{X}_1, \ldots, \boldsymbol{X}_N$ to solve the stochastic program from Eq.(83) with $\boldsymbol{w} = \hat{\boldsymbol{v}}_{ti-1}$. Denote the solution by $\hat{\boldsymbol{v}}_{ti}$;
4. If $\hat{\gamma}_{ti} < \gamma$ set the counter $ti = ti + 1$ and reiterate from Step 2; otherwise, proceed with Step 5 ;
5. Let $T = ti$ be the final iteration counter. Generate $\boldsymbol{X}_1, \ldots, \boldsymbol{X}_{N_1} \sim iid\ f(\cdot; \hat{\boldsymbol{v}}_T)$ and estimate ℓ via importance sampling as in 82, with $\boldsymbol{u} = \hat{\boldsymbol{v}}_T$.

Algorithm reproduced integrally from (BOTEV et al., 2013).

3.4.5 Cross-entropy algorithm for optimization

Let $\mathcal{J}$ be a real-valued performance function in $\mathbb{R}^n$. Suppose one wants to find the maximum of $\mathcal{J}$ in the set $\mathbb{R}^n$, and $\boldsymbol{x}^\star$ corresponds to the achieved maximum. Being the maximum given by γ^* (KROESE; TAIMRE; BOTEV, 2011),

$$\mathcal{J}(\boldsymbol{x}^*) = \gamma^* = \max_{\boldsymbol{x} \in \mathbb{R}^n} \mathcal{J}(\boldsymbol{x}) \ . \tag{84}$$

Associating it with the probability estimation problem, $\ell = \mathcal{P}(\mathcal{J}(\boldsymbol{X}) \geq \gamma)$, where $\boldsymbol{X}$ has some PDF $f(x; \boldsymbol{u})$ in $\mathbb{R}^n$. If γ is a near-unknown choice γ^*, it is typically the probability of a rare-event, and the CE approach for estimation can be used to search for the distribution of importance sampling near the sampling density of theoretical greatest importance, which concentrates all its mass on the point X^* (KROESE; TAIMRE; BOTEV, 2011).

Sampling from this distribution produces optimal or close to optimal results. The main difference with CE for the simulation of a rare-event is that in the optimization setting the final level, $\gamma = \gamma^*$, is not known in advance. The CE produces, for optimization, a sequence of levels $\hat{\gamma}_{ti}$ and reference parameter $\boldsymbol{v}_{ti}$ such the level tends to the ideal γ^* and $\boldsymbol{v}_{ti}$ to the ideal $\boldsymbol{v}^*$, corresponding to the point $\boldsymbol{X}^*$ (KROESE; TAIMRE; BOTEV, 2011).

Given the sample size N^s and the parameter ϱ, in according with (BOTEV et al., 2013),

CE Algorithm for optimization

1. Choose an initial parameter vector $\boldsymbol{v}_0$. Let $N^e = [\varrho N^s]$.
Set t = 1.(iteration counter) ;

2. Generate $\boldsymbol{X}_1, \ldots, \boldsymbol{X}_N \sim$ iid. Calculate $\mathcal{J}_i = \mathcal{J}(\boldsymbol{X}_i)$
for all i, and order these from smallest to largest: $\mathcal{J}_{(1)} \leq \ldots \leq \mathcal{J}_{(N)}$. Let $\hat{\gamma}_{ti}$
be the sample $(1 - \varrho)$ - quantile of performances; that is,
$\hat{\gamma}_{ti} = \mathcal{J}_{(N^s - N^e + 1)}$.

3. Use the same sample $\boldsymbol{X}_1, \ldots, \boldsymbol{X}_N$ to solve the stochastic program

$$\max_{\boldsymbol{v}} \frac{1}{N} \sum_{X_k \epsilon \mathcal{E}}^{N} \ln f(\boldsymbol{X}_k; \boldsymbol{v})$$

Denote the solution by $\hat{\boldsymbol{v}}_{ti}$;

4. If some stopping criterion is met, stop; otherwise, set $ti = ti + 1$, and return to Step 2.

Algorithm reproduced integrally from (BOTEV et al., 2013).

Note that the estimate of step 5 is missing from the algorithm because in the optimization configuration the estimation of ℓ does not matter. For the same reason, it does not have the likelihood ratio $W(\boldsymbol{X}_k; \boldsymbol{u}, \boldsymbol{v})$ in the problem for the step 3 (BOTEV et al., 2013).

A smoothing updating rule is used, in which the vector $\hat{\boldsymbol{v}}_{ti}$ is

$$\hat{\boldsymbol{v}}_{ti} = \alpha \hat{\boldsymbol{v}}_{ti} + (1 - \alpha) \hat{\boldsymbol{v}}_{ti-1} \ , \tag{85}$$

where $\hat{\boldsymbol{v}}_{ti}$ is the solution of Eq.(85) and α is the smoothing parameter, which can vary between 0 and 1 (typically between 0.7 and 1). The smoothing effect is discussed in detail in the work of (COSTA; JONES; KROESE, 2007). In particular, it is shown that the appropriate smoothing of the CE that converges and finds a good one is close to 1 (usually

0.9). When this parameter is large, it generates a convergence for degenerate distribution, which can happen quickly, which would “freeze” the algorithm in a suboptimal solution. To avoid this, another form of smoothing is also used (KROESE; TAIMRE; BOTEV, 2011) ,

$$\beta_{ti} = \beta - \beta \left(1 - \frac{1}{\mathrm{ti}}\right)^{\vartheta} \tag{86}$$

where ϑ is a small integer (typically between 5 and 10), β is a large smoothing constant (typically between 0.8 and 0.99) (KROESE; TAIMRE; BOTEV, 2011).

If the problem of optimization has constraints, the constraints are defined by the inequality (BOTEV et al., 2013),

$$q_i(\boldsymbol{X}) \leq 0 \ , \ i = 1, \ldots, K. \tag{87}$$

Two approaches can be used: acceptance-rejection (RUBISTEIN; KROESE, 2004) and penalization. In the optimization problems addressed in this dissertation, only penalization is used. In penalization, the objective function is modified to

$$\tilde{\mathcal{J}}(\boldsymbol{X}) = \mathcal{J}(\boldsymbol{X}) + \sum_{i=1}^{K} \nu_i \max\{q_i(\boldsymbol{X}), 0\} \ , \tag{88}$$

where $\nu_i < 0$ measures the importance (cost) of the ith penalty (BOTEV et al., 2013).

3.5 Example with a simple function

One wants to maximize the objective function, given by

$$\mathcal{J}(x_1, x_2) = 3(1 - x_1)^2 \ e^{-x_1^2-(x_2+1)^2} - 10\left(\frac{x_1}{5} - x_1^3 - x_2^5\right) e^{-x_1^2-x_2^2} - \frac{1}{3} \ e^{-(x_1+1)^2-x_2^2} \ . \tag{89}$$

The Figure 9 shows the graph of the function (89), considering the domain $-3 \leq x_1 \leq 3$ and $-3 \leq x_2 \leq 3$.

Figure 9 - Illustration of objective function with two variables plotted in 3D.

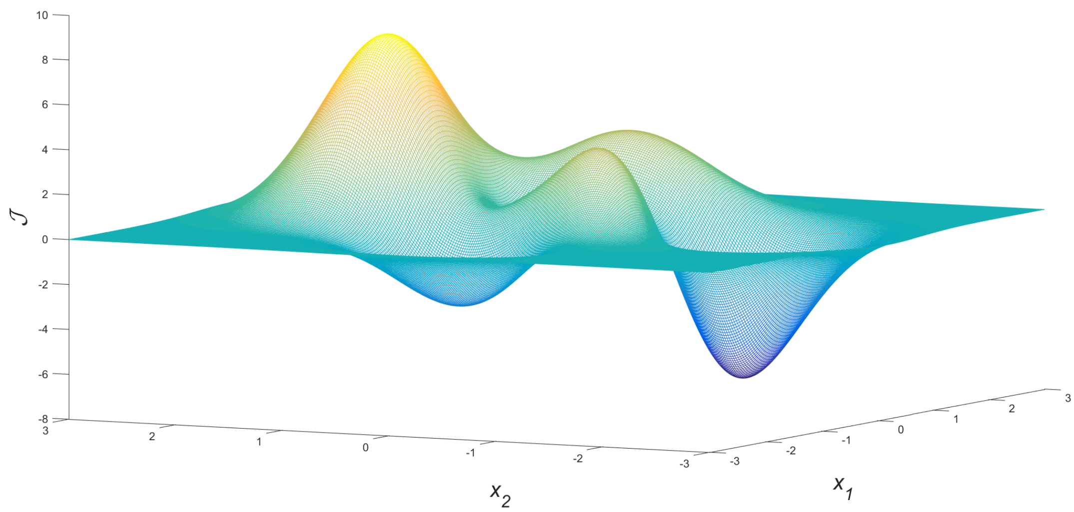

It is possible to note that $\mathcal{J}(x_1, x_2)$ is near of 8, in this specified range for x_1 and x_2. Table 1 shows the results found by three optimization methods approached in this chapter, SQP, GA and CE, applied for maximization of this objective function, with initial point $x_0 = [-2.8 \ \ -2.8]$. For each optimization method, the value of the objective function $\mathcal{J}$ is presented along the variables x_1, x_2 and the number of evaluations of the function (Func. Eval.).

Table 1 - Results found by SQP, GA and CE in a simple objective function without constraint.

Method	$\mathcal{J}$	x_1	x_2	Func. Eval.
SQP	8.1	0	1.58	33
GA	8.1	0	1.58	1525
CE	8.1	0	1.58	625

In SQP, the objective function gradient is reported and $\texttt{tol} = 10^{-4}$. The other parameters values used are default to MATLAB. In GA, $Ps = 25$, $p_e = 0.1$ and $\texttt{tol} = 10^{-4}$. The other parameters values used are default to MATLAB. For comparative purposes, in the CE, $N^s = 25$, $\varrho = 0.1$, $\texttt{tol} = 10^{-4}$.

The three methods arrive at the same value of the objective function, at the maximum point of the function in that interval. The CE needing less function evaluations (Func. Eval.) than GA.

The Figure 10 shows the way travelled by the three optimization methods on the axis x_1 and x_2.

Figure 10 - Illustration of objective function with two variables plotted in 2D.

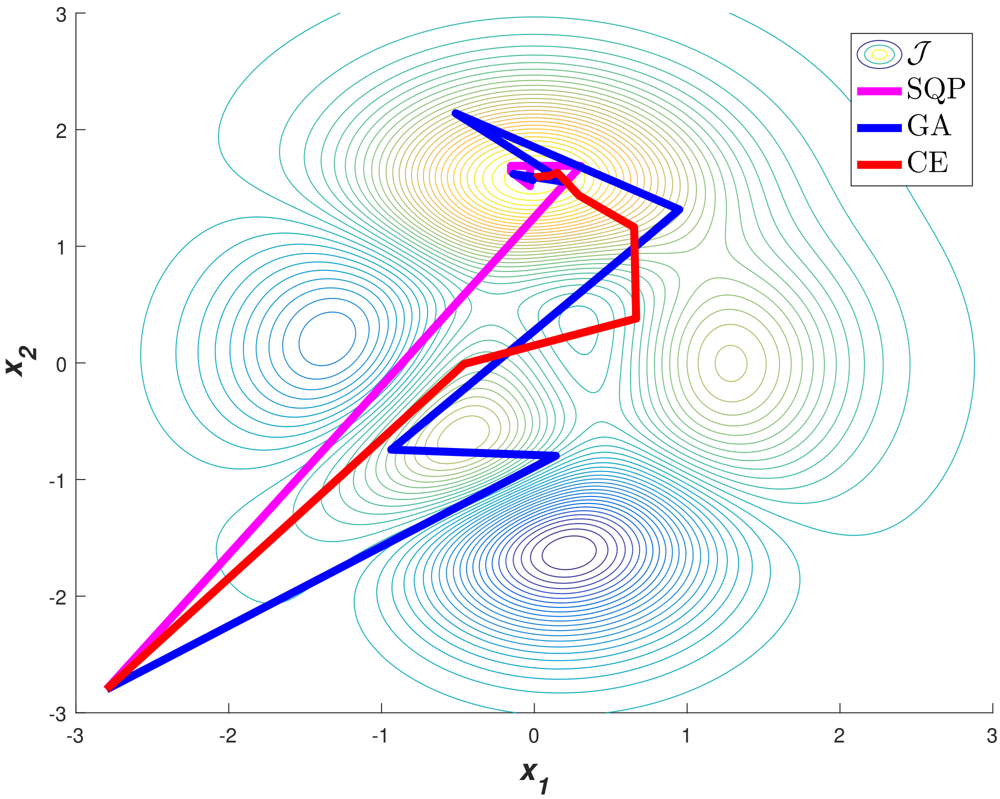

At each iteration, GA generates population and CE generates samples. In Figure 10, the curves plotted by the GA and CE paths are the values of the population averages for GA and the average samples for CE, generated in each iteration. The Table 2 shows how the CE behaves in each iteration, updating the parameters like the mean (μ) and standard deviation (s), while converging to the maximum of the objective function.

Table 2 - CE values in each iteration in objective function simple.

t	$\mathcal{J}$	μ_1	μ_2	s_1	s_2
1	2.270146794	-0.459488051	-0.008968961	3.355055509	3.249769611
2	2.860637918	0.666141420	0.380440439	1.354542286	1.366441447
3	4.120106677	0.653027829	1.162957566	0.470619301	0.606686539
4	7.008146053	0.292017193	1.435687713	0.205226793	0.315769793
5	7.446003646	0.208695935	1.552400068	0.163201844	0.127856667
6	7.787336640	0.150389597	1.631149240	0.072993344	0.058795721
7	8.026009241	0.087775724	1.599568535	0.044001077	0.027193471
8	8.042151458	0.065650017	1.604063321	0.027625736	0.023088652
9	8.083833389	0.039167002	1.595569159	0.015990682	0.008429217
10	8.096324708	0.018816278	1.594326504	0.010926462	0.005318778
11	8.101883225	0.011828933	1.591081221	0.003974162	0.003303728
12	8.102966154	0.009470405	1.587883017	0.001917568	0.001899837
13	8.103276289	0.008622787	1.586882162	0.001050735	0.001376096
14	8.103513239	0.007690584	1.586595490	0.000714133	0.000765119
15	8.103689691	0.006903584	1.586423788	0.000593667	0.000288602
16	8.103927300	0.006181502	1.586305936	0.000460310	0.000242046
17	8.104050961	0.005799505	1.586206148	0.000242446	0.000224023
18	8.104080980	0.005554602	1.586130823	0.000104673	0.000205486
19	8.104097370	0.005516682	1.586056304	0.000130614	0.000186414
20	8.104156944	0.005428984	1.585846654	0.000093632	0.000173132
21	8.104198108	0.005353612	1.585647122	0.000060946	0.000163367
22	8.104232821	0.005284162	1.585569881	0.000036286	0.000094541

The three optimization methods found the same maximum value. Note that, in this problem with a simple objective function without constraint, it can be said that the CE is faster than the GA. In this dissertation, the results obtained in the numerical experiments will all be discussed and commented in this manner.

4 NUMERICAL EXPERIMENTS

This chapter presents the numerical results of this dissertation. Four trusses are presented in this dissertation, where in the first truss the design variables are the internal diameter d_i and height H, and in the second truss, d_i and thickness t. In the third truss, the design variables are the cross-section area A of each bar and the constraints are, in the first case, the yield stress and, in the second case, the natural frequencies. In the fourth truss the design variables are d_i and t, at two heights (h_1 and h_2), considering scenarios with and without buckling stress as constraints by checking the maximum displacement allowed in the nodes.

4.1 **Truss 1 - 2 bars and 3 nodes**

The Figure 11 shows the truss 1 with a cross-section representation depicting its symmetry and normal force $\mathcal{N}$ in each element and angle θ.

Figure 11 - Physical model of the Truss 1.

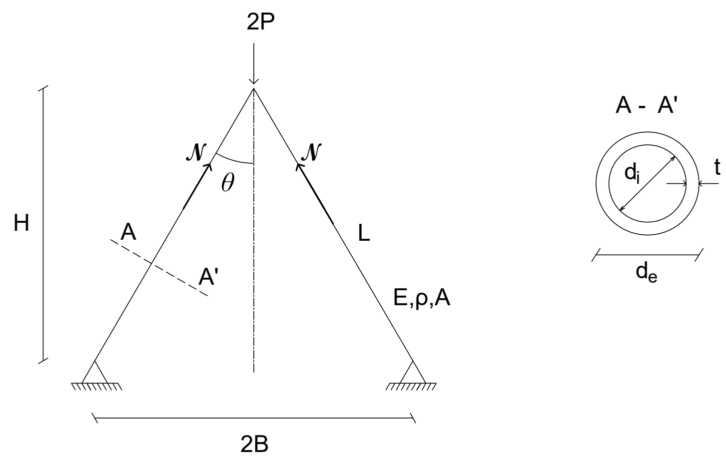

Source: (FOX, 1977)

Considering the structural bars as tubular, the design variables in this case are the internal diameter d_i and height H, and a “minimum weight” is sought while the stresses in the bars are smaller than yield stress S_y and of buckling σ_E, also respecting the structural integrity criteria.

Let ρ be the density, B the base half, P the applied load half, d_e the external diameter, t the thickness and E the Young's modulus, being all these variables with known values. The objective optimization is weight minimization changing d_i and H. Due to the symmetry and simplicity of the Truss 1, the stresses in the bars are equal ($\sigma_1 = \sigma_2 = \sigma$), as well as the critical buckling stress in each bar ($\sigma_1^E = \sigma_2^E = \sigma^E$), and mass, stresses, and constraints are found by expressions different from those shown in section 2.5. The two stresses are compressible and equal. Therefore when considering the buckling stress as constraints, these two stress are considered. Being m the objective function, and x the design variables, the optimization problem is defined as

$$\boxed{\begin{array}{l} \quad \min_{\boldsymbol{x}} m = \sum_{e=1}^{2} \rho A_e(\boldsymbol{x}) L_e(\boldsymbol{x}), \qquad \boldsymbol{x} = \{d_i, H\}\ , \\ \text{where} \\ \quad 20mm \leq d_i \leq 50mm\ , \\ \quad 500mm \leq H \leq 1000mm\ , \\ \text{subject to} \\ \quad \sigma \leq S_Y \text{ (yield stress constraint)}, \\ \quad \sigma \leq \sigma^E \text{ (buckling constraint)}. \end{array}} \tag{90}$$

The weight m of this model with two bars is given by

$$m = 2\rho V\ , \tag{91}$$

where V is the volume of each bar. The volume can be written as $V = AL$, where A is the cross-section and L is the bar length, which are obtained by the expressions

$$A = (d_e^2 - d_i^2)\pi/4 = [(d_i + 2t)^2 - d_i^2]\pi/4 = (d_i\, t + t^2)\pi\ , \tag{92}$$

$$L = \sqrt{B^2 + H^2}\ . \tag{93}$$

Thus, mass can be expressed by equation

$$m = 2\rho\pi(d_i\, t + t^2)\sqrt{B^2 + H^2}\ . \tag{94}$$

The force $\mathcal{N}$, the angle θ and P are related in the expression,

$$2P = 2\mathcal{N}\cos\theta = 2\mathcal{N}\frac{B}{\sqrt{B^2 + H^2}}. \tag{95}$$

The stress σ in the bar depends of force $\mathcal{N}$. So that

$$\sigma = \frac{\mathcal{N}}{A} = \frac{P\sqrt{B^2 + H^2}}{H\pi\,(d_i\, t + t^2)}\ . \tag{96}$$

The inertial moment I is obtained by expression

$$I = \frac{\pi}{64}(d_e^4 - d_i^4)\ . \tag{97}$$

With this, using the Eq.(22), the critical buckling stress for this case is

$$\sigma^E = \frac{\pi^2 E((d_i + 2t)^4 - d_i^4)}{16\,(B^2 + H^2)\,(4\,d_i\,t + 4t^2)}\ . \tag{98}$$

For nominal conditions, the design variables are assumed as equal to $(d_i, H) = (50, 1000)\ mm$. The considered yield stress is $S_Y = 250MPa$ in each bar. The following values are fixated: $P = 25KN$, $E = 210GPa$, $B = 1.5m$, $t = 5mm$ and $\rho = 7900\ kg/m^3$. The total mass of the truss in this case is $m = 24.6\ kg$. The Table 4.1 has results in nominal conditions.

Table 3 - Stresses at each bar of the two-dimensional truss with nominal conditions in Truss 1.

d_i (mm)	H (mm)	mass (kg)	σ (MPa)	σ^E (MPa)	S_Y (MPa)
50	1000	24.6	-52	267	250

No structural integrity criteria are violated at the nominal condition, as can be noted in Table 4.1. This problem can be solved by finding the solution of the lattice for a sequence of pairs (d_i,H) within the established limits until one knows to update the weight to the minimum. For small problems with few variations, this procedure is possible. The structural optimization in this case is of size and shape.

For comparison with the CE, other optimization methods are used. One gradient-based method, the SQP, and a zero-order metaheuristic, the GA.

In the SQP, the Matlab function called fmincon (find minimum of constrained nonlinear multivariable function) is used. It is a nonlinear programming solver. Using fmincon of the Matlab, the SQP algorithm is selected.

A parameter analysis is done with the SQP, GA and CE parameters, to identify how the parameter individually affects the operation of these numerical methods. This parameter analysis is done in this structural model because it is simpler than the others explored in this dissertation. It is in the appendix of this dissertation.

The start points for the three methods are the middle points of the optimization problem range.

4.1.1 Optimization with yield stress constraint

In the SQP, the objective function gradient and constraints are reported and `tol` $= 10^{-4}$. The others parameters values are the default of MATLAB.

In general, GA parameters are the number of population, number of generations, elite count, crossover fraction and mutation beyond the method convergence criteria. Consider the GA parameters, Ps is the population size, E_C is the elite count where $E_C = p_e Ps$, p_e is the percentage of the population size used in the elite count ($0 \leq p_e \leq 1$), and finally the crossover fraction. In this case, GA control parameters are $Ps = 25$, $E_C = 4$, cross fraction over is 0.8 (MATLAB default) and `tol` $= 10^{-4}$. The others parameters values are the default of MATLAB.

The number of samples N^s, the elite number of samples N^e, tolerance `tol` and number of maximum iterations l_{max} are parameters that need to be defined in the beginning of the CE Algorithm for optimization. In this case, CE control parameters are $N^s = 25$, $N^e = 4$, `tol` $= 10^{-4}$ and $l_{max} = 100$. Table 4 shows the results of the three methods (SQP, GA and CE) for the stresses.

Note that all results respect the constraint $\sigma \leq S_Y$. They come close to violating the yield stress, because the optimization methods try to reduce the mass to the maximum without violating the restrictions. Reducing the mass, increases the stress in the structure. The SQP and GA arrive at the same value for d_i, and the σ in GA is most distant of S_Y. In the Table 5 one has the results showing the mass and function evaluations (Func. Eval.).

Table 4 - Stress at each bar with values found by optimization methods, not considering buckling, for Truss 1.

Method	d_i (mm)	H (mm)	σ (MPa)
SQP	20.0	395	250
GA	20.0	458	218
CE	20.1	431	231

Table 5 - Comparison between the results obtained with different optimization techniques, not considering buckling, in Truss 1.

Method	mass (kg)	d_i (mm)	H (mm)	Func. Eval.
SQP	9.6	20.0	395	6
GA	9.7	20.0	458	3925
CE	9.7	20.1	431	325

Note that the found values are different in the three optimization methods. The values found by CE are better than GA, and CE is faster than GA, because the CE needs fewer function evaluations (Func. Eval.). The mass is the same in GA and CE.

The Figure 12 shows the contour plot, demonstrating how the mass and σ are changing according to the variables d_i and H, and also showing the solution points that are in accord with the optimization problem constraints, where the masses is slightly smaller than $m = 10\ kg$. The Figure 13 shows that in the last iteration all the samples are concentrated at the same point, very close to the SQP, where this point is the solution found by the CE.

Figure 12 - Contour plot of mass and σ in function of the d_i and H of the Truss 1 with the values found by optimization methods.

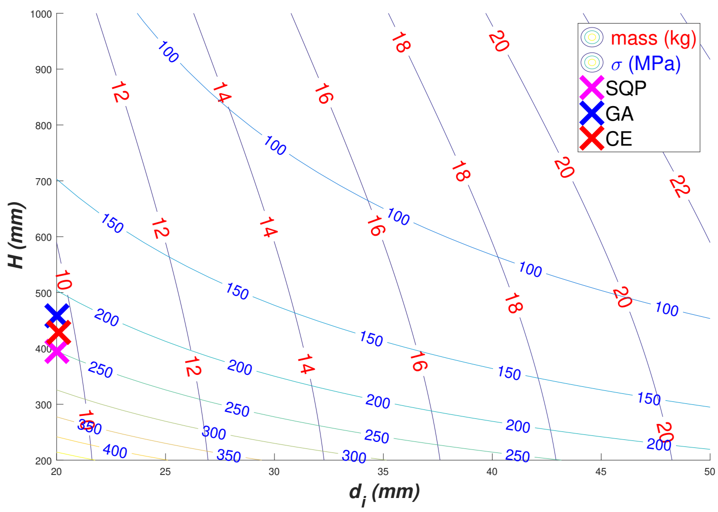

The Figure 13 shows the behavior of the CE samples converging to the solution according to each iteration. The solution found by SQP is marked with the color magenta. The number of stop iterations is denoted l_{stop}.

Figure 13 - Illustration of CE sampling of the domain at different levels (iterations), not considering buckling, of the Truss 1. The magenta cross is the SQP reference solution.(CE control parameters are $N^s = 25$, $N^e = 4$, $\texttt{tol} = 10^{-4}$, $l_{stop} = 13$ and $l_{max} = 100$)

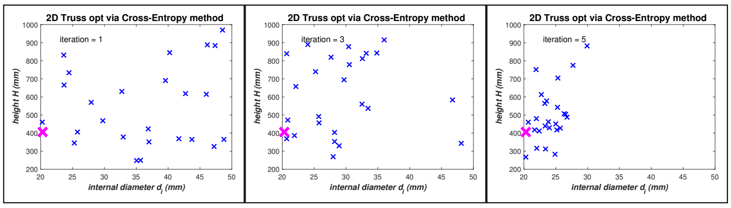

(a) level $l = 1$ (b) level $l = 3$ (c) level $l = 5$

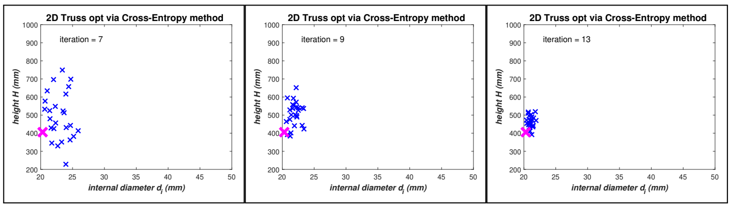

(d) level $l = 7$ (e) level $l = 9$ (f) level $l = 13$

4.1.2 Optimization with yield stress and buckling limit constraints

Structural optimization considering buckling becomes a stringent test for the numerical methods.

In the SQP, the objective function gradient and constraints are reported with $\texttt{tol} = 10^{-4}$. The GA control parameters are $Ps = 25$, $E_C = 17$ and $\texttt{tol} = 10^{-4}$. The others parameters values are the default of MATLAB. The CE control parameters are $N^s = 50$, $N^e = 15$, $\texttt{tol} = 10^{-4}$ and $l_{max} = 100$.

The Table 6 has the results obtained by the optimization methods. Note that all results respect the constraint $\sigma \leq \sigma^E$. The buckling stress changes with changes of the design variables that are optimized. The CE finds the same mass as the GA, but the Func. Eval. and CPU Time in the CE is smaller than in GA, as shown in the Table 7.

The Figure 14 shows how the mass, σ and σ^E are changing according with the variables d_i and H, and the points that represent the solutions found by the optimization methods. It is possible to note that the solution found in the CE is closer than that of the SQP and more distant than that of the GA, and that the solutions found by the three optimization methods are on the same line that represents the $m = 14\ kg$.

The Figure 15 shows the behavior of the CE according to the iterations considering buckling. In the last iteration all the samples are concentrated at the same point, very close to the SQP, where the mean of this point is the solution found by the CE.

Table 6 - Stress at each bar with values found by optimization methods considering buckling of the Truss 1.

Method	d_i (mm)	H (mm)	σ (MPa)	σ^E (MPa)
SQP	29.1	674	114	114
GA	30.2	576	126	127
CE	29.4	659	115	117

Table 7 - Comparison between the results obtained with different optimization techniques considering buckling in Truss 1.

Method	mass (kg)	d_i (mm)	H (mm)	Func. Eval.
SQP	13.9	29.1	674	19
GA	14.0	30.2	576	8550
CE	14.0	29.4	659	3850

Figure 14 - Contour plot of mass, σ_{VM} and σ_E in function of the d_i and H of the Truss 1.

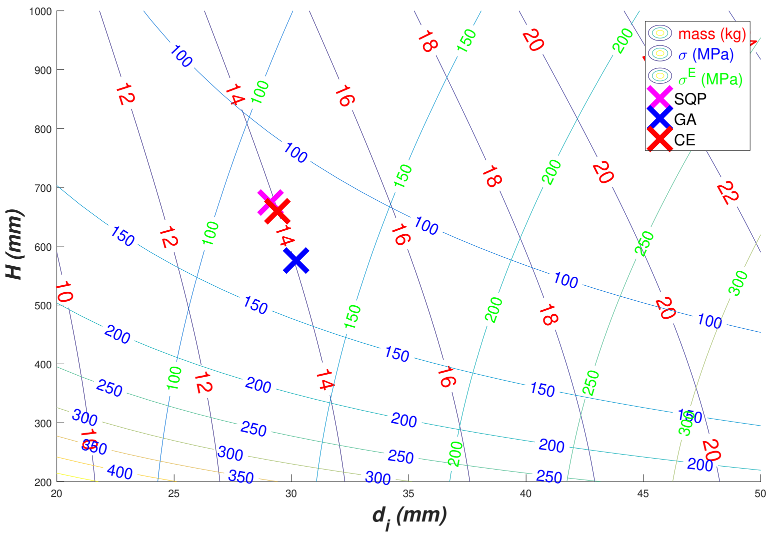

Figure 15 - Illustration of CE sampling of the domain at different levels (iterations) considering buckling of the Truss 1. The magenta cross is the SQP reference solution. (CE control parameters are $N^s = 50$, $N^e = 15$, $\texttt{tol} = 10^{-4}$, $l_{stop} = 77$ and $l_{max} = 100$)

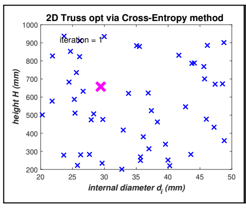

(a) level $l = 1$

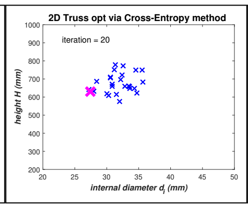

(b) level $l = 20$

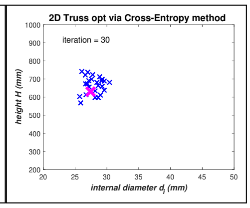

(c) level $l = 30$

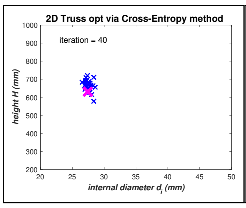

(d) level $l = 40$

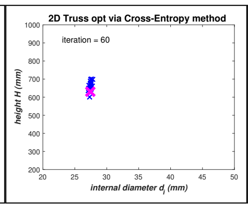

(e) level $l = 60$

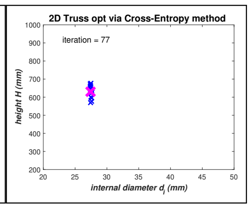

(f) level $l = 77$

4.2 **Truss 2 - 11 bars and 6 nodes**

The Truss 2 consists in 11 bars connected through 6 nodes, as shown in Figure 16.

Figure 16 - Physical model of the Truss 2.

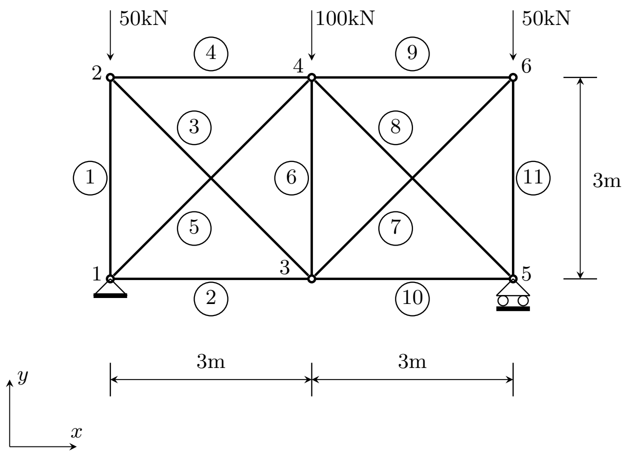

Source: (FERREIRA, 2009)

Note that due to kinematic constraints, $u_1 = v_1 = v_5 = 0$ (Eq. 27), $N = 11$ and $f_4 = f_{12} = -50kN$ and $f_8 = -100kN$ (Eq. 28). The optimization problem is defined as

$$
\boxed{\begin{array}{l}
\quad \min_{\boldsymbol{x}} m = \sum_{e=1}^{11} \rho A_e(\boldsymbol{x}) L_e, \qquad \boldsymbol{x} = \{d_i, t\} \ , \\
\text{where} \\
\quad 20mm \leq d_i \leq 100mm \ , \\
\quad 3mm \leq t \leq 20mm \ , \\
\text{subject to} \\
\quad |\sigma| \leq S_Y \text{ (yield stress constraint)}, \\
\quad \sigma^c \leq \sigma^E \text{ (buckling constraint)}.
\end{array}} \tag{99}
$$

It is needed to consider fix parameter values like $E = 290GPa$, $S_Y = 25MPa$ and $\rho = 7900\ kg/m^3$. Considering the nominal values with these parameters, $d_i = 100\ mm$ and $t = 20\ mm$, the mass in this conditions is $m = 2262\ kg$. The Table 8 shows the stress state with nominal values to check if they are close to the applied constraints. In nominal conditions, the criterion of structural integrity is not violated, as can be noted in Table 8. The start points for the three methods are the middle points of the optimization problem range.

Table 8 - Stresses at each bar in initial conditions of the Truss 2.

bar	1	2	3	4	5	6	7	8	9	10	11
σ (MPa)	-8	5	3	-2	-7	-4	3	-7	-2	5	-8
σ^E (MPa)	426	426	213	426	213	426	213	213	426	426	426

4.2.1 Optimization with yield stress constraint

Considering the yield stress constraint, in the SQP, the objective function gradient and constraints are reported with $\texttt{tol} = 10^{-4}$. The GA control parameters are $Ps = 25$, $E_C = 3$ and $\texttt{tol} = 10^{-4}$. The others parameters values are the default of MATLAB. The CE control parameters are $N^s = 25$, $N^e = 3$, $\texttt{tol} = 10^{-4}$ and $l_{max} = 100$. The Table 9 has the results.

Table 9 - Comparison between the results obtained with different optimization techniques, not considering buckling, in Truss 2.

Method	mass (kg)	d_i (mm)	t (mm)	Func. Eval.
SQP	78	20.0	3.5	5
GA	78	20.0	3.5	2657
CE	78	20.0	3.5	175

Note, in the Table 9, that all methods arrived at the same optimal value. The CE being faster (Func. Eval. smaller) than the GA, but being slower than the SQP, which is a gradient-based method.

The Table 10 shows the stress state with the optimal values of the variables found by the three optimization methods. Note that all stresses in the bars are less than $S_Y = 250MPa$. This means that the optimization respects the imposed structural integrity constraint.

Table 10 - Stresses at each bar with variables found by SQP, GA and CE method (equals) in Truss 2.

bar	1	2	3	4	5	6	7	8	9	10	11
σ (MPa)	-245	142	73	-51	-201	-103	73	-201	-51	142	-245

The Figure 17 shows how the samples converge to the optimal point, where the behavior of the CE in each iteration is observed. In the last iteration, all samples are concentrated at the optimum point, in this case.

Figure 17 - Illustration of CE sampling of the domain at different levels (iterations) of the Truss 2. The magenta cross is the SQP reference solution, not considering buckling. (CE control parameters are $N^s = 25$, $N^e = 3$, $\texttt{tol} = 10^{-4}$, $l_{stop} = 7$ and $l_{max} = 100$)

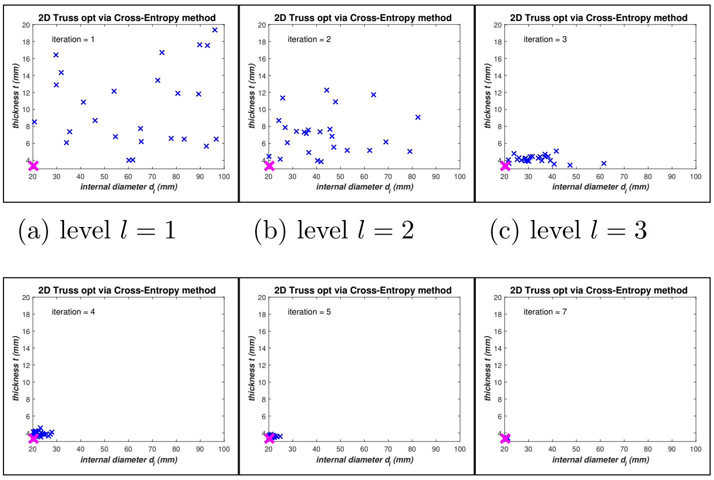

(a) level $l = 1$ (b) level $l = 2$ (c) level $l = 3$

(d) level $l = 4$ (e) level $l = 5$ (f) level $l = 7$

4.2.2 Optimization with yield stress and buckling limit constraints

Considering yield stress and buckling limit constraints, the GA control parameters are changed to $Ps = 50$ and $E_C = 15$, and CE control parameters to $N^s = 50$ and $N^e = 15$. The Table 11 has the results.

Table 11 - Comparison between the results obtained with different optimization techniques considering buckling in Truss 2.

Method	mass (kg)	d_i (mm)	t (mm)	Func. Eval.
SQP	205	69.6	3.0	21
GA	209	68.7	3.1	5250
CE	207	69.9	3.0	2200

The CE found the same value of the SQP, being faster than the GA. The Table 12, Table 13 and Table 14 show the stress state with the optimal values of the variables by SQP, GA CE.

No stress exceeded the critical buckling stress when the stresses are compressive ($\sigma < 0$), respecting the criterion of structural integrity, as show the Table 12, Table 13 and Table 14. The Figure 18 shows the behavior of the CE according to the iterations considering buckling. The samples are very close to the optimum and little dispersed.

Table 12 - Stresses at each bar with variables found by SQP method considering buckling in Truss 2.

bar	1	2	3	4	5	6	7	8	9	10	11
σ (MPa)	-92	54	27	-19	-76	-39	27	-76	-19	54	-92
σ^E (MPa)	152	152	76	152	76	152	76	76	152	152	152

Table 13 - Stresses at each bar with variables found by GA method considering buckling in Truss 2.

bar	1	2	3	4	5	6	7	8	9	10	11
σ (MPa)	-90	52	27	-19	-74	-38	27	-74	-19	52	-90
σ^E (MPa)	149	149	74	149	74	149	74	74	149	149	149

Table 14 - Stresses at each bar with variables found by CE method considering buckling in Truss 2.

bar	1	2	3	4	5	6	7	8	9	10	11
σ (MPa)	-92	54	27	-19	-76	-39	27	-76	-19	54	-92
σ^E (MPa)	152	152	76	152	76	152	76	76	152	152	152

Figure 18 - Illustration of CE sampling of the domain at different levels (iterations) of the Truss 2. The magenta cross is the SQP reference solution considering buckling. (CE control parameters are $N^s = 50$, $N^e = 15$, $\texttt{tol} = 10^{-4}$, $l_{stop} = 40$ and $l_{max} = 100$)

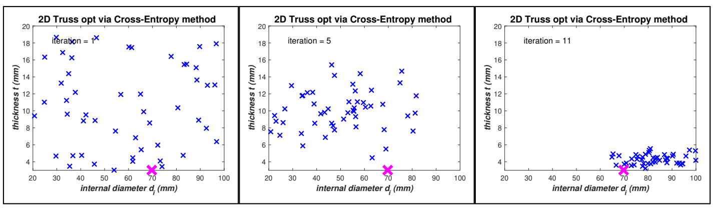

(a) level $l = 1$ (b) level $l = 5$ (c) level $l = 11$

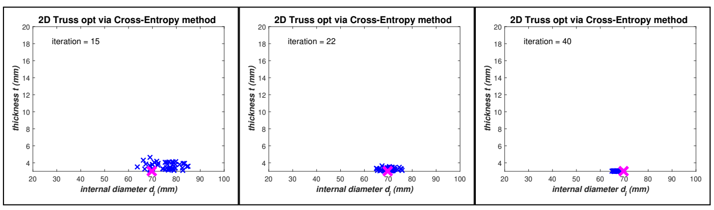

(d) level $l = 15$ (e) level $l = 22$ (f) level $l = 40$

4.3 Truss 3 - 10 bars with 6 nodes

The Truss 3 consists of 10 bars connected through 6 nodes, as shown in Figure 19.

Figure 19 - Physical model of the Truss 3.

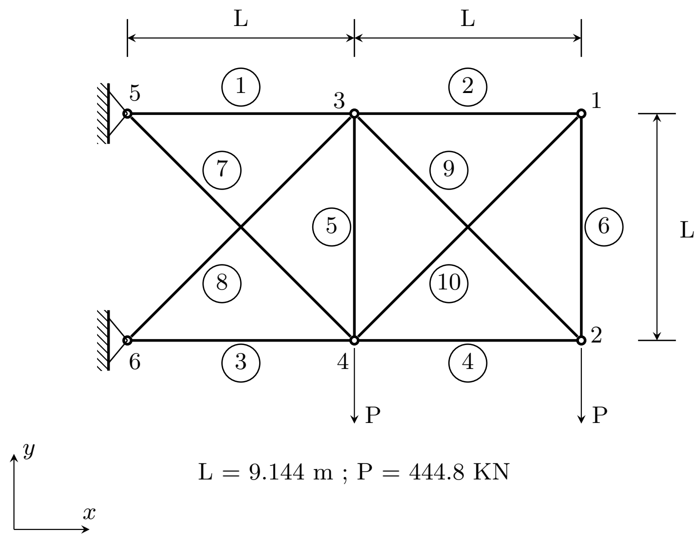

Source: (HAFTKA; GÜRDAL, 1992)

This problem is based on Haftka's example (HAFTKA; GÜRDAL, 1992). Note that due to kinematic constraints, $u_5 = v_5 = u_6 = v_6 = 0$ (Eq. 27), $N = 10$ and $f_4 = f_8 = -P$ (Eq. 28). The optimization problem is defined as

$$\boxed{\begin{array}{l} \quad \min_{\boldsymbol{x}} m = \sum_{e=1}^{10} \rho A_e L_e, \qquad \boldsymbol{x} = \{A_e\} \ , \\ \text{where} \\ \quad 65\ mm^2 \leq A_e \leq 12903\ mm^2 \ , \\ \text{subject to} \\ \quad |\sigma| \leq S_Y \text{ (yield stress constraint)}, \\ \quad \text{If } e = 9,\ S_Y = 517\ MPa\text{; else, } S_Y = 172\ MPa. \end{array}} \tag{100}$$

It is needed fixate parameters values like $E = 68.9\ GPa$, $L = 9.144\ m$, $P = 444.8\ kN$ and $\rho = 2770\ kg/m^3$. $S_Y = 172\ MPa$ for all members except bar 9. For bar 9, $S_Y = 517\ MPa$. These values are chosen following the Haftka reference (HAFTKA; GÜRDAL, 1992), and in this book are in English units. Considering the nominal values with these parameters, $A_e = 12903\ mm^2$ for all areas, the mass in this conditions is $m = 3807\ kg$. In nominal conditions, the criterion of structural integrity is not violated, as can be noticed in Table 15. The Table 15 shows the stress state with nominal values to check that they are close to the applied constraints. The start points for the three methods are the middle points of the optimization problem range.

Table 15 - Stresses at each bar in nominal conditions in Truss 3.

bar	1	2	3	4	5	6	7	8	9	10
σ (MPa)	67	14	-71	-21	12	14	51	-47	29	-20
S_Y (MPa)	172	172	172	172	172	172	172	172	517	172

4.3.1 Optimization of cross-sectional areas with yield stress constraint

In the SQP, the objective function gradient and constraints are reported, using `tol` $= 10^{-4}$. The GA control parameters are $Ps = 50$, $E_C = 15$ and `tol` $= 10^{-4}$. The other parameter values are the default of MATLAB. The CE control parameters are $N^s = 50$, $N^e = 15$, `tol` $= 10^{-4}$ and $l_{max} = 300$.

Table 16 - Comparison between the results obtained with different techniques optimizing the area of each bar in Truss 3.

Method	mass (kg)	Func. Eval.
SQP	679	12
GA	701	49930
CE	689	5950

In this case, the $l_{stop} = 238$. The results found by SQP are identical to those found in Haftka's book (HAFTKA; GÜRDAL, 1992), which in the book are in English units. The CE gets closer to SQP and is faster than GA. In the Tables 17, 18 and 19 one can be seen if the constraint are respected.

Table 17 - Values at each bar with variables found by SQP method in Truss 3.

bar	1	2	3	4	5	6	7	8	9	10
$A_e(mm^2)$	5097	65	5526	2516	65	65	3741	3558	2372	91
σ (MPa)	172	172	-172	-172	0.01	172	172	-172	259	-172

Table 18 - Values at each bar with variables found by GA method in Truss 3 .

bar	1	2	3	4	5	6	7	8	9	10
$A_e(mm^2)$	4962	289	5564	2319	68	300	4086	3307	2251	401
σ (MPa)	170	167	-169	-171	1.00	161	171	-170	250	-170

Table 19 - Values at each bar with variables found by CE method in Truss 3.

bar	1	2	3	4	5	6	7	8	9	10
$A_e(mm^2)$	5099	80	5529	2518	65	80	3765	3560	2374	113
σ (MPa)	172	172	-163	-172	-5.6	172	172	-171	257	-171

Note that all methods met the structural integrity criterion imposed in the structural optimization, where the CE came closer to the SQP. The Table 20 shows an illustration of the areas obtained by the three optimization methods.

Table 20 - Illustration of the areas obtained by the three optimization methods considering yield stress constraint in Truss 3.

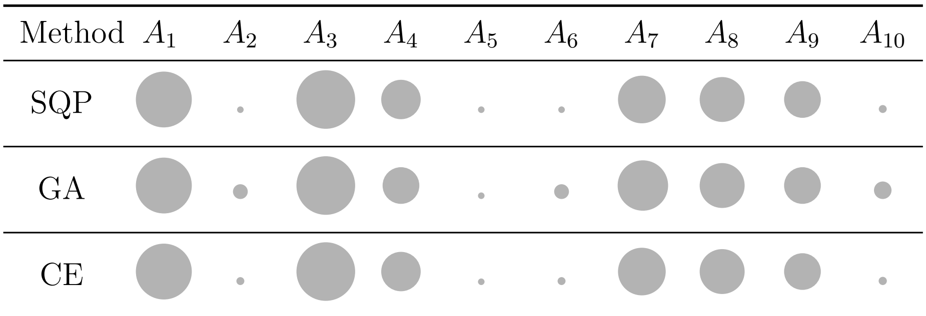

4.3.2 Optimization with natural frequency constraints

The natural frequency is also a criterion of structural integrity that can be used as a constraint for structural optimization. The structural model must have values of natural frequencies bigger or equal from defined values, such as $\omega_1^* = 7\ Hz$, $\omega_2^* = 15\ Hz$ and $\omega_3^* = 20\ Hz$, with an added mass m_{ad} of 454 kg, so that resonance does not occur.

The design variables are the ten areas. The new range and added mass value are based on Ho-Huu's article (HO-HUU et al., 2016). The optimization problem is redefined as

$$\boxed{\begin{array}{l} \quad \min_{\boldsymbol{x}} m = \sum_{e=1}^{10} \rho A_e L_e, \qquad \boldsymbol{x} = \{A_e\}\ , \\ \text{where} \\ \quad 65.4\ mm^2 \leq A_e \leq 5000\ mm^2\ , \\ \quad m_{ad} = 454\ kg, \\ \text{subject to} \\ \omega_1 \geq 7\ Hz,\ \omega_2 \geq 15\ Hz \text{ and } \omega_3 \geq 20\ Hz. \end{array}} \tag{101}$$

Considering that in the nominal conditions all the transverse areas of the bars have the same value $A_e = 5000\ mm^2$, one has the natural frequencies in the Table 21.

Table 21 - Natural frequencies in the Truss 3 with nominal parameters in Hz.

ω_1	ω_2	ω_3	ω_4	ω_5	ω_6	ω_7	ω_8
15.0	43.0	51.4	99.5	102.4	117.6	124.0	150.3

By reducing the cross-sectional areas and consequently the mass of the structural system, with the natural frequency values defined to be used as constraints, it reduces the mass of the structural system as much as possible until the natural frequency gets bigger or equal to the values defined as constraint.

In the SQP, the objective function gradient and constraints are reported with `tol` $= 10^{-8}$. The GA control parameters are $Ps = 50$, $E_C = 10$ and `tol` $= 10^{-8}$. The other parameter values are the default of MATLAB. The CE control parameters are $N^s = 50$, $N^e = 10$, `tol` $= 10^{-8}$ and $l_{max} = 100$. The Table 22 has the results.

In this case, $l_{stop} = 96$. The Table 23 shows the areas found by the optimization methods. The Table 24 shows an illustration of the areas obtained by the three optimization methods. The Table 25 shows the natural frequencies found by the optimization methods. Note that all optimization methods have respected the constraints, with the first three natural frequencies ω_1, ω_2 and ω_3 being greater than the constraints ω_1^*, ω_2^* and ω_3^*.

Table 22 - Comparison between the results obtained with different techniques optimizing the area of each bar in Truss 3.

Method	mass (kg)	Func. Eval.
SQP	530	313
GA	529	9836
CE	535	4800

Table 23 - Values of cross-sectional area in the Truss 3 found by optimization methods in mm^2.

Method	A_1	A_2	A_3	A_4	A_5	A_6	A_7	A_8	A_9	A_{10}
SQP	3813	1800	3777	980	435	415	2380	1981	1132	1373
GA	3210	1507	3678	1314	79	493	2652	2210	1359	1282
CE	3581	1197	3308	1661	145	532	2230	2707	1448	1179

Table 24 - Illustration of the areas obtained by the three optimization methods considering natural frequencies constraint in Truss 3.

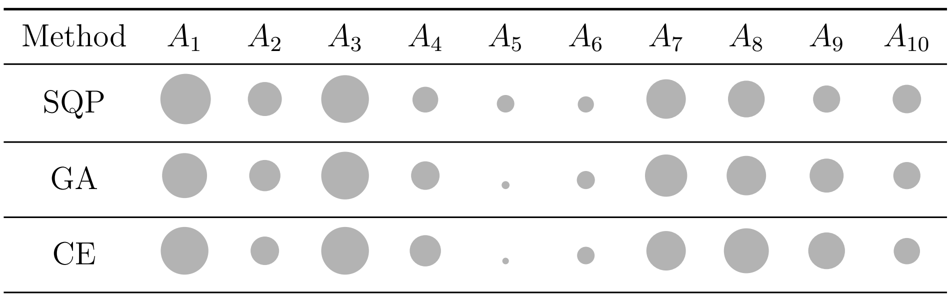

Table 25 - Natural frequencies in the Truss 3 found by optimization methods in Hz.

Method	ω_1	ω_2	ω_3	ω_4	ω_5	ω_6	ω_7	ω_8
SQP	7.0	17.6	20.0	20.0	28.2	31.1	47.7	52.3
GA	7.0	16.2	20.0	20.3	29.1	29.5	48.1	50.8
CE	7.0	16.8	20.1	21.0	28.5	30.5	48.1	51.1

Dynamic constraints also can be used in structural optimization. Local search algorithms are not suitable in this type of optimization problem. Only global search algorithms should be used to obtain optimal solutions for these situations (MIGUEL; MIGUEL, 2012). In general, the SQP obtains better results than the GA and the CE. However, in this case, where the constraints are the natural frequencies, the metaheuristic, GA, obtain better results than those of SQP, which is a gradient-based optimization method, and CE has a satisfactory result, as shown in the Table 25.

Miguel's article (MIGUEL; MIGUEL, 2012) presents two new metaheuristic methods developed in the last decade: Harmony Search (HS) and Firefly Algorithm (FA). These two optimization methods are applied in this optimization problem with constraints on the natural frequencies being a nonlinear dynamic optimization problem. In this article, is the first time that these two methods are used in sizing and shape optimization with natural frequencies constraints, in according with (MIGUEL; MIGUEL, 2012). The Table 26 has the results of the two methods and of the CE.

The Table 27 shows the areas found by the optimization methods CE, HS, and FA. The Table 28 shows an illustration of the areas obtained by these three optimization methods and the Table 29 shows the natural frequencies. The values of HS and FA are from Miguel's article (MIGUEL; MIGUEL, 2012).

Table 26 - Comparison between the results obtained by CE, HS and FA optimizing the area of each bar in Truss 3.

Method	mass (kg)	Func. Eval.
CE	535	4800
HS	535	20000
FA	531	5000

Table 27 - Values of cross-sectional area in the Truss 3 found by optimization methods CE, HS and FA in mm^2.

Method	A_1	A_2	A_3	A_4	A_5	A_6	A_7	A_8	A_9	A_{10}
CE	3581	1197	3308	1661	145	532	2230	2707	1448	1179
HS	3428	1565	3764	1606	107	474	2250	2460	1287	1210
FA	3620	1403	3475	1490	65.4	467	2347	2551	1271	1235

Table 28 - Illustration of the areas obtained by CE, HS and FA considering natural frequencies constraint in Truss 3.

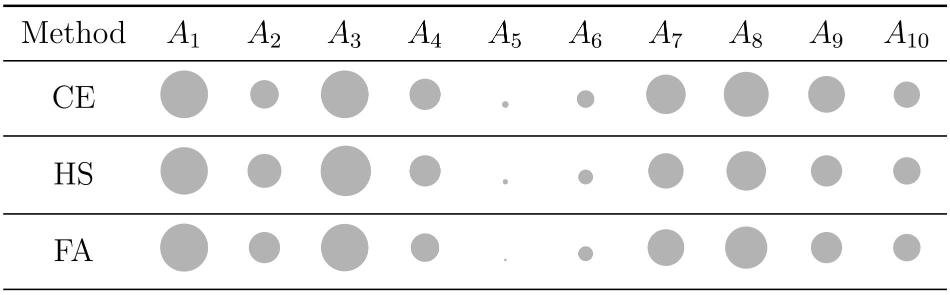

Table 29 - Natural frequencies in the Truss 3 found by optimization methods CE, HS and FA in Hz.

Method	ω_1	ω_2	ω_3	ω_4	ω_5	ω_6	ω_7	ω_8
CE	7.0	16.8	20.1	21.0	28.5	30.5	48.1	51.1
HS	7.0	16.7	20.1	20.3	28.5	29.3	49.0	51.7
FA	7.0	16.1	20.0	20.0	28.5	28.9	48.3	50.8

The CE presents the same HS mass with smaller function evaluation number (Func. Eval.). The FA presents a mass better than of CE and almost the same function evaluation number. CE, HS, and FA are optimization methods considered news and for this, can be improved and in the future present better results in this example. HS and FA are not gradient-based and FA comes close to the SQP in the value of mass, even though FA has the Func. Eval. much bigger, comparing with SQP. Although CE does not find a better solution than other methods in this case, the CE finds a satisfactory solution with a smaller function evaluation number (Func. Eval.), confirming its efficiency and viability as a technique for structural optimization.

4.4 **Truss 4 - 15 bars and 8 nodes**

The truss 4 consists of 15 bars connected through 8 nodes, as shown in Figure 20.

Figure 20 - Physic model of the Truss 4.

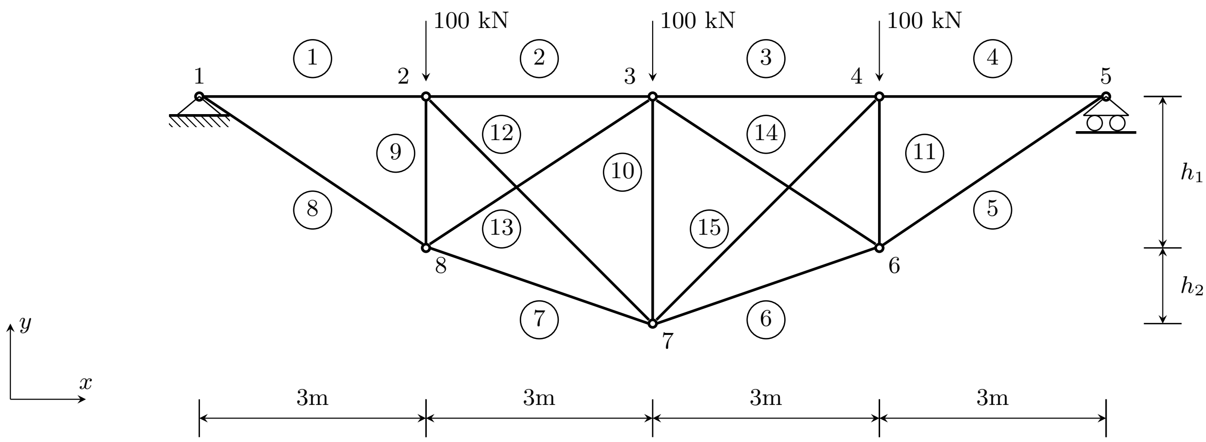

Source: (KALANTA et al., 2012)

Note that due to kinematic constraints, $u_1 = v_1 = v_6 = 0$ (Eq. 27), $N = 15$ and $f_4 = f_6 = f_8 = -100kN$ (Eq. 28).

The optimization problem is defined as

$$
\boxed{
\begin{array}{l}
\quad \min_{\boldsymbol{x}} m = \sum_{e=1}^{15} \rho A_e(\boldsymbol{x}) L_e(\boldsymbol{x}), \qquad \boldsymbol{x} = \{d_i, t, h_1, h_2\} \ , \\
\text{where} \\
\quad 50\ mm \leq d_i \leq 100\ mm \ , \\
\quad 10\ mm \leq t \leq 20\ mm, \\
\quad 1000\ mm \leq h_1 \leq 2000\ mm, \\
\quad 100\ mm \leq h_2 \leq 1000\ mm, \\
\text{subject to} \\
\quad |\sigma| \leq S_Y \text{ (yield stress constraint)}, \\
\quad \sigma^c \leq \sigma^E \text{ (buckling constraint)}.
\end{array}
}
\tag{102}
$$

It is needed to consider fix parameter values like $E = 290GPa$, $S_Y = 250MPa$ and $\rho = 7900kg/m^3$. Considering the nominal values with these parameters, $d_i = 100\ mm$, $t = 20\ mm$, $h_1 = 2000\ mm$ and $h_2 = 1000\ mm$, the mass in this conditions is $m = 3352\ kg$. The Table 30 shows stresses in each bar in the nominal conditions. In nominal conditions, the criterion of structural integrity is not violated, as can be noted in Table 30.

Table 30 - Stresses at each bar in initial conditions in Truss 4.

bar	1	2	3	4	5	6	7	8	9	10	11	12	13	14	15
σ (MPa)	-30	-27	-27	-30	36	31	31	-36	-10	-13	-10	-4	0.3	0.3	-4
σ^E (MPa)	588	588	588	588	407	530	530	407	1324	588	1324	294	407	407	294

4.4.1 Optimization with yield stress constraint

Considering the yield stress constraint, in the SQP, the objective function gradient and constraints are not reported, with `tol` $= 10^{-4}$. The GA control parameters are $Ps = 25$, $E_C = 5$ and `tol` $= 10^{-4}$. The other parameter values are the default of MATLAB. The CE control parameters are $N^s = 25$, $N^e = 5$, `tol` $= 10^{-4}$ and $l_{max} = 100$. The Table 31 has the results.

In this case, $l_{stop} = 59$. All optimization methods found the same value of internal diameter, which in this case is the minimum limit for this design variable, and the value of h_1. CE is faster than GA and provides less mass than GA. The Tables 32, 33 and 34 show the stresses with the optimal values. These Tables show that the constraint $S_Y = 250\ MPa$ is respected.

Table 31 - Comparison between the results obtained with different optimization techniques, not considering buckling, optimizing d_i, t, h_1 and h_2 in Truss 4.

Method	mass (kg)	d_i (mm)	t (mm)	h_1 (m)	h_2 (m)	Func. Eval.
SQP	602	50.0	10.0	1.01	0.24	20
GA	609	50.0	10.1	1.01	0.21	3973
CE	608	50.0	10.1	1.01	0.18	1250

Table 32 - Stresses at each bar with variables found by SQP method, not considering buckling, optimizing d_i, t, h_1 and h_2 in Truss 4.

bar	1	2	3	4	5	6	7	8	9	10	11	12	13	14	15
σ (MPa)	-237	-244	-244	-237	250	250	250	-250	-57	-46	-57	7	-13	-13	7

Table 33 - Stresses at each bar with variables found by GA method, not considering buckling, optimizing d_i, t, h_1 and h_2 in Truss 4.

bar	1	2	3	4	5	6	7	8	9	10	11	12	13	14	15
σ (MPa)	-233	-242	-242	-233	246	249	249	-247	-56	-42	-56	10	-16	-16	10

Table 34 - Stresses at each bar with variables found by CE method, not considering buckling, optimizing d_i, t, h_1 and h_2 of the Truss 4.

bar	1	2	3	4	5	6	7	8	9	10	11	12	13	14	15
σ (MPa)	-234	-247	-247	-234	247	250	250	-247	-57	-39	-58	14	-20	-20	15

4.4.2 Optimization with yield stress and buckling limit constraints

Considering yield stress and buckling limit constraints, in the SQP, the objective function gradient and constraints are not reported, with `tol` $= 10^{-4}$. The GA control parameters are $Ps = 25$, $E_C = 3$ and `tol` $= 10^{-4}$. The other parameter values are the default of MATLAB. The CE control parameters are $N^s = 25$, $N^e = 3$, `tol` $= 10^{-4}$ and $l_{max} = 100$. The Table 35 has the results.

In this case, the $l_{stop} = 38$. The CE is faster than GA and has a mass less than GA. The Tables 36, 37 and 38 show the stresses with the optimal values.

Table 35 - Comparison between the results obtained with different optimization techniques considering buckling and optimizing d_i, t, h_1 and h_2 of the Truss 4.

Method	mass (kg)	d_i (mm)	t (mm)	h_1 (m)	h_2 (m)	Func. Eval.
SQP	815	68.5	10.0	1.32	0.10	56
GA	856	71.2	10.5	1.01	0.10	2625
CE	852	69.1	10.3	1.2	0.49	950

Table 36 - Stresses at each bar with variables found by SQP method considering buckling and optimizing d_i, t, h_1 and h_2 in Truss 4.

bar	1	2	3	4	5	6	7	8	9	10	11	12	13	14	15
σ (MPa)	-138	-152	-152	-138	151	158	158	-151	-47	-23	-47	15	-21	-21	15
σ^E (MPa)	180	180	180	180	151	180	180	151	931	804	931	147	151	151	147

Table 37 - Stresses at each bar with variables found by GA method considering buckling and optimizing d_i, t, h_1 and h_2 in Truss 4.

bar	1	2	3	4	5	6	7	8	9	10	11	12	13	14	15
σ (MPa)	-165	-181	-181	-165	174	185	185	-174	-43	-24	-43	17	-21	-21	17
σ^E (MPa)	195	195	195	175	195	195	175	1723	1427	1723	172	175	175	175	172

Table 38 - Stresses at each bar with variables found by CE method considering buckling and optimizing d_i, t, h_1 and h_2 in Truss 4.

bar	1	2	3	4	5	6	7	8	9	10	11	12	13	14	15
σ (MPa)	-146	-140	-140	-146	157	146	146	-157	-36	-40	-36	-7	-2	-2	-7
σ^E (MPa)	185	185	185	185	159	178	159	1153	581	1153	140	159	159	159	140

4.4.3 Optimization subject to maximum displacement

In this section, the maximum displacement is considered as a constraint for structural optimization. The maximum displacement value is $d_{p_{max}} = 50\ mm$. The nominal values are considered, with the following parameters: $d_i = 100\ mm$, $t = 20\ mm$, $h_1 = 2000\ mm$ and $h_1 = 1000\ mm$, for the displacements in each node, as shows in the Table 39. Due kinematic constraints, $u_1 = v_1 = v_6 = 0$. So, $d_{p_1} = 0$.

With the FEA, it is possible to observe how the structural model behaves due to vertical load, as shown in Figure 21, where the blue line represents the nominal condition of the structural model and the red dashed line represents the deformed structural model.

In the SQP, the objective function gradient and constraints are not reported, with $\texttt{tol} = 10^{-4}$. The GA control parameters are $Ps = 25$, $E_C = 3$ and $\texttt{tol} = 10^{-4}$. The others parameters values are the default of MATLAB. The CE control parameters are $N^s = 25$, $N^e = 3$, $\texttt{tol} = 10^{-4}$ and $l_{max} = 100$. The Table 40 shows the results. The Table 41 shows the displacements of each node with the values of the design variables optimized by the optimization methods.

Table 39 - Displacements in each node of the Truss 4 in nominal conditions.

node	1	2	3	4	5	6	7	8
d_{p_n} (mm)	0	3.0	3.5	3.2	1.6	2.9	3.3	3.1

Figure 21 - Displacements of the Truss 4.

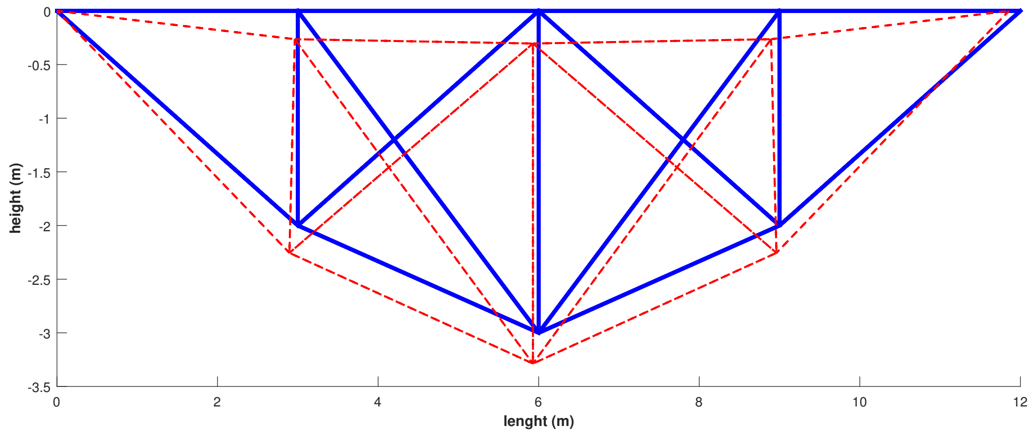

Table 40 - Comparison between the results obtained with different optimization techniques subject to maximum displacement optimizing d_i, t, h_1 and h_2 in Truss 4.

Method	mass (kg)	d_i (mm)	t (mm)	h_1 (m)	h_2 (m)	Func. Eval.
SQP	602	50.0	10.0	1.04	0.16	35
GA	613	50.0	10.0	1.20	0.11	2699
CE	606	50.2	10.1	1.20	0.19	475

Table 41 - Displacement of each node in mm using the values found by the optimization methods of the Truss 4.

Method	d_{p1}	d_{p2}	d_{p3}	d_{p4}	d_{p5}	d_{p6}	d_{p7}	d_{p8}
SQP	0	40.0	50.0	41.2	13.5	39.8	49.8	40.8
GA	0	31.6	40.1	32.8	11.9	31.3	39.9	32.4
CE	0	39.5	48.9	40.6	13.4	39.2	48.7	40.2

In this case, $l_{stop} = 19$. The CE is faster than the GA and finds a better value in the objective function than the GA. Note that the displacements nodes do not exceed the maximum displacement, $d_{p_{max}} = 50\ mm$, respecting the constraint, as shown the Table 41.

CONCLUDING REMARKS

This chapter recalls the main topics addressed in this dissertation, highlighting its contributions and suggesting future works.

Thematic addressed

This work is motivated by the importance of structural optimization in the context of Engineering and in the world, and the continuous search for new numerical methods for this type of optimization.

In this context, the dissertation proposes a new framework for structural optimization based on CE, a relatively new metaheuristic that has was successfully used in simulation of rare events and combinatorial optimization. To the best of the author's knowledge, there is only one work where this optimization method is used in structural optimization (GHIDEY, 2015).

Four structural models are used, with FEA being implemented before beginning the structural optimization processes. For comparative analysis, in addition to CE, two more methods of numerical optimization are presented: SQP, which is gradient-based, and GA, which is a metaheuristic based on Darwin's theory of evolution (DARWIN, 2009). Therefore, in all structural models three optimization methods are used, SQP, GA and CE.

Conclusions and contributions

The dissertation presents the following contributions:(i) the development of the mathematical formalism necessary to formulate the problem of structural optimization, as well as the analysis of the new numerical procedure; (ii) The implementation of the new numerical method in a computational code in written Matlab language; (iii) a detailed analysis on the accuracy and efficiency of this new framework.

The constraints of structural optimization problems are the structural integrity criteria addressed in this dissertation, such as yield stress, buckling stress, natural frequencies and displacement. Before mentioning these constraints for structural optimization, the concept of solid mechanics is presented, such as the balance of continuous mechanics equations and boundary conditions, which needs to be considered for structural optimization.

A generic formulation of an optimization problem is also made and the mathematical approach of the three methods used, SQP, GA and CE, is presented following the nomenclature of the initial generic formulation.

Numerical experiments evaluate the effectiveness and robustness of the cross-entropy method in the context of structural optimization. The results show that the evaluated method is very competitive, having a much better performance than genetic algorithm, proving to be an appealing tool for optimization problems, especially when the use of gradients is impractical.

It is important to mention that in all cases, the optimal values found by the CE are close to those found by the SQP, being SQP a first-order method and CE a zero-order method. Like SQP, which uses the gradient in its computational process, first-order methods will in general be more efficient (better results) and faster than the CE for convex problems. When comparing CE with another zero-order method, GA, it is noted that in most case the CE is faster and obtains better results than the GA in the numerical experiments and implementations presented in this work, making the CE quite interesting for application in structural optimization.

It can be noticed that even with high computational resources, it is always necessary to have a good professional or researcher who can analyze the data and interpret them so that this information is not misused. The study of buckling stresses with the optimization process requires greater attention due to the non convexity.

Suggestions for future works

In this dissertation, CE is used in two types of structural optimization, size and shape. Size optimization changes the sizing, such as cross-sections and other internal dimensions of structural components. Shape optimization changes the shape of a structure to solve the problem in the best way.

For these reasons, the following is suggested for future works: (i) application of CE in topological optimization, where in topological optimization all definitions are based on model analysis and the final result is the optimal material distribution; (ii) application of CE in 3D structural models for optimization.

Publication

During his master, the author, with his advisors and other collaborator published an article in *Proceeding Series of the Brazilian Society of Computational and Applied Mathematics* and presented the work at the congress *XXXVIII Congresso Nacional de Matemática Aplicada e Computacional* (ISSA et al., 2018).

REFERENCES

AKBARI, J.; SADOUGHI, A. Shape optimization of structures under earthquake loadings. *Structural and Multidisciplinary Optimization*, v. 47, n. 6, p. 855–866, 2013.

AL-BAALI, M.; FLETCHER, R. An efficient line search for nonlinear least squares. *Journal of Optimization Theory and Applications*, v. 48, n. 3, 1986.

BEKDAS S. M. NIGDELI, X. Y. G. Sizing optimization of truss structures using flower pollination algorithm. *Applied Soft Computing*, v. 37, p. 322–331, 2015.

BOER, P. D.; KROESE, D. P.; MANNOR, S.; RUBINSTEIN, R. Y. A tutorial on the cross-entropy method. *Annals of Operations Research*, v. 134, p. 19–67, 2005.

BOGGS, P. T.; TOLLE, J. W. Sequential quadratic programming for large-scale nonlinear optimization. *Journal of Computational and Applied Mathematics*, v. 124, p. 123–127, 2000.

BOGOMOLNY, M.; BENDSOE, M.; HATTEL, J. H. A shape optimization study for tool design in resistance welding. *Structural and Multidisciplinary Optimization*, v. 38, n. 2, p. 185–194, 2009.

BONNANS, J. F.; GILBERT, J. C.; LEMARECHAL, C.; SAGASTIZÁBAL, C. A. *Numerical Optimization: Theoretical and Practical Aspects*. 2nd. ed. New York, USA: Springer, 2009.

BOTEV, Z. I.; KROESE, D. P.; RUBINSTEIN, R. Y.; L'ECUYER, P. The cross-entropy method for optimization. *Handbook of Statistics*, v. 31, p. 35–59, 2013.

BROYDEN, C. G. The convergence of a class of double-rank minimization algorithms. *IMA Journal of Applied Mathematics*, v. 6, p. 76–90, 1970.

BRUNO, H. *Shape Optimization with Symmetric Galerkin Boundary Element Method*. Master Dissertation — Pontifícia Universidade Católica do Rio de Janeiro, 2017.

CAVAGNA S. RICCI, L. R. L. Structural sizing, aeroelastic analysis, and optimization in aircraft conceptual design. *Journal of Aircraft*, v. 48, n. 6, p. 1840–1855, 2011.

CAVAZZUTI, M. et al. High performance automotive chassis design: A topology optimization based approach. *Structural and Multidisciplinary Optimization*, v. 44, n. 1, p. 45–56, 2010.

CHAOVALITWONGSE, W. A.; CHOU, C. A.; LIANG, Z.; WANG, S. Applied optimization and data mining. *Annals of Operations Research*, v. 249, n. 1-3, p. 1–3, 2017.

CHRISTENSEN, P. W.; KLARBRING, A. *An Introduction to Structural Optimization*. Van Godewijckstraat, Dordrecht, Netherlands: Springer, 2009. v. 153.

CHUN, J.; SONG, J.; PAULINO, G. H. System-reliability-based design and topology optimization of structures under constraints on first-passage probability. *Structural Safety*, v. 76, p. 81–94, 2019.

COSTA, A.; JONES, O. D.; KROESE, D. Convergence properties of the cross-entropy method for discrete optimization. *Operations Research Letters*, n. 35, p. 573 – 580, 2007.

CUELLAR, N.; PEREIRA, A.; MENEZES, I. F. M.; CUNHA Jr, A. Non-intrusive polynomial chaos expansion for topology optimization using polygonal meshes. *Journal of the Brazilian Society of Mechanical Sciences and Engineering*, v. 40, p. 561, 2018.

CUNHA Jr, A. *Modeling and Uncertainty Quantification in the Nonlinear Stochastic Dynamics of a Horizontal Drillstrings*. Tese (D.Sc. Thesis) — Pontifícia Universidade Católica do Rio de Janeiro / Université Paris-Est, 2015.

CUNHA Jr, A.; SOIZE, C.; SAMPAIO, R. Computational modeling of the nonlinear stochastic dynamics of horizontal drillstrings. *Computational Mechanics*, p. 849–878, 2015.

DANILO, O.; GIRALDO, M. Solving a classical optimization problem using gams optimizer package: Economic dispatch problem implementation. *Ingeniería y Ciencia*, v. 13, n. 26, 2017.

DARWIN, C. *The Origin of species: by means of natural Selection, or the preservation of favoured races in the struggle for life*. 6th. ed. New York, USA: Cambridge University Press, 2009.

DAVIDON, W. C. Variable metric method for minimization. *SIAM Journal on Optimization*, v. 1, n. 1, p. 1–17, 1991.

DEATON, J. D.; GRANDHI, R. V. A survey of structural and multidisciplinary continuum topology optimization: post 2000. *Structural and Multidisciplinary Optimization*, v. 49, n. 1, p. 1–38, 2014.

EBY, D. J.; AVERILL, R.; GOODMAN, E.; SIDHU, R. Shape optimization crashworthy structures. In: 7TH INTERNATIONAL LS-DYNA USERS CONFERENCE. Detroit, Michigan, USA, 2002.

FERREIRA, A. J. M. *MATLAB Codes for Finite Element Analysis Solids and Structures*. Van Godewijckstraat, Dordrecht, Netherlands: Springer, 2009. v. 153.

FLETCHER, R. A new approach to variable metric algorithms. *The Computer Journal*, v. 13, p. 317–322, 1970.

FLETCHER, R.; MAZA, E. S. Nonlinear programming and nonsmooth optimization by successive linear programming. *Mathematical Programming: Series A and B*, v. 43, n. 1-3, 1989.

FLOUDAS, C. A.; PARDALOS, P. M. (Ed.). *Encyclopedia of Optimization*. 2nd. ed. New York, USA: Springer, 2009.

FOX, J. A. *Hydraulic Analysis of Unsteady Flow in Pipe Networks*. London, UK: Macmillan Education, 1977.

GHASEMI, M.; DIZANGIAN, B. Size, shape and topology optimization of composite steel box girders using pso method. *Asian Journal of Civil Engineering (Building and Housing)*, v. 11, n. 6, p. 699–715, 2010.

GHIDEY, H. *Reliability-based design optimization with Cross-Entropy method*. Master Dissertation — Norwegian University of Science and Technology, 2015.

GOLDBERG, D. E. *Genetic algorithms in search, optimization and machine learning*. Boston, Massachusetts, USA: Addison-Wesley Publishing Company, Inc., 1989.

GOLDFARB, D. A family of variable-metric methods derived by variational means. *Mathematics of Computation*, v. 24, n. 109, p. 23–26, 1970.

GRIHON, S. Structure sizing optimization capabilities at airbus. 12th World Congress on Structural and Multidisciplinary Optimisation. 2017.

HADDOCK, J.; MITTHENTAL, J. Simulation optimization using simulated annealing. *Computers & Industrial Engineering*, v. 22, n. 4, p. 387–395, 1992.

HAFTKA, R. T.; GRANDHI, R. V. Structural shape optimization - a survey. *Computer Methods in Applied Mechanics and Engineering*, v. 57, n. 1, p. 91–106, 1986.

HAFTKA, R. T.; GÜRDAL, Z. *Element of Structural Optimization*. 3rd. ed. Dordrecht, Netherlands: Kluwer Publishers, 1992.

HJELMSTAD, K. D. *Fundamentals of Structural Mechanics*. 2nd. ed. New York, USA: Springer, 2005.

HO-HUU, V.; VO-DUY, T.; LUU-VAN, T.; LE-ANH, L.; NGUYEN-THOI, T. Optimal design of truss structures with frequency constraints using improved differential evolution algorithm based on an adaptive mutation scheme. *Automation in Construction*, v. 68, p. 81–94, 2016.

HOLLAND, J. H. *Adaptation in Natural and Artificial Systems*. Cambridge, UK: The MIT Press, 1992.

HORCAIO, J. T. Real-time simulation and optimization parametric tests applied to competition: The bmw team brazil case. In: SAE BRAZIL. Campinas-SP, Brazil, 2013.

HSU, Y. A review of structural shape optimization. *Computers in Industry*, v. 25, p. 3–13, 1994.

IRGENS, F. *Continuum Mechanics*. Heidelberg, Germany: Springer, 2008.

ISSA, M. V. S.; CUNHA Jr, A.; SOEIRO, F. J. C. P.; PEREIRA, A. Structural optimization using the cross-entropy method. In: XXXVIII CONGRESSO NACIONAL DE MATEMÁTICA APLICADA E COMPUTACIONAL. Campinas-SP, Brazil, 2018.

JONES, R. M. *Deformation Theory of Plasticity*. Blacksburg, Virginia, USA: Bull Ridge Publishing, 2009.

KALANTA, S.; ATKOČIŪNAS, J.; ULITINAS, T.; GRIGUSEVIČIUS, A. Optimization of bridge trusses height and bars cross-sections. *The Baltic Journal of Road and Bridge Engineering*, v. 7, n. 2, p. 112–119, 2012.

KENNEDY, J.; EBERHART, R. Particle swarm optimization. *Proceedings of ICNN'95 - International Conference on Neural Networks*, 1995.

KHARE, A.; RANGNEKAR, S. A review of particle swarm optimization and its applications in solar photovoltaic system. *Applied Soft Computing*, v. 13, 2013.

KRAMER, O. *Genetic Algorithm Essentials*. Gewerbestrasse, Switzerland: Springer, 2017.

KROESE, D. P.; BRERETON, T.; TAIMRE, T.; BOTEV, Z. I. Why the monte carlo method is so important today. *Wiley Interdisciplinary Reviews: Computational Statistics*, v. 6, n. 6, p. 386–392, 2014.

KROESE, D. P.; POROTSKY, S.; RUBINSTEIN, R. Y. The cross-entropy method for continuous multi-extremal optimization. *Methodology and Computing in Applied Probability*, v. 8, n. 3, p. 383–407, 2006.

KROESE, D. P.; RUBINSTEIN, I. C. R. Y.; POROTSKY, S.; TAIMRE, T. Cross-entropy method. *Encyclopedia of Operations Research and Management Sciences*, Springer, n. 3, p. 326–333, 2013.

KROESE, D. P.; TAIMRE, T.; BOTEV, Z. I. *Handbook of Monte Carlo Methods*. Hoboken, New Jersey: Wiley, 2011.

LAGAROS, N. D.; PAPADRAKAKIS, M.; KOKOSSALAKIS, G. Structural optimization using evolutionary algorithms. *Computers and Structures*, v. 80, p. 571–589, 2002.

LEE, K. S.; GEEM, Z. W. A new meta-heuristic algorithm for continuous engineering optimization: harmony search theory and practice. *Computer Methods in Applied Mechanics and Engineering*, v. 194, n. 36-38, p. 3902–3933, 2005.

LEITE, J. P. B.; TOPPING, B. H. V. Parallel simulated annealing for structural optimization. *Computers and Structures*, v. 73, n. 1-5, p. 545–564, 1999.

LIANG, Y. C.; JUAREZ, J. R. C. A novel metaheuristic for continuous optimization problems: Virus optimization algorithm. *Engineering Optimization*, Taylor & Francis, v. 48, n. 1, p. 73–93, 2015.

LOPES, M. A. *Otimização estrutural de uma fundação de concreto armado submetida a solicitações dinâmicas provenientes de um conjunto motor-compressor de alta capacidade*. Master Dissertation — Universidade do Estado do Rio de Janeiro, 2017.

MAROS, I. *Computational Techiniques of the Simplex Method*. 1st. ed. Norwell, Massachusetts, USA: Kluwer Academic Publishers, 2013.

MENDONÇA, F. G. *Otimização Estrutural de Torres de Aço para Suporte de Turbinas Eólicas utilizando a Interface MATLAB-ANSYS*. Master Dissertation — Universidade do Estado do Rio de Janeiro, 2017.

MIGUEL, L. F. F.; MIGUEL, L. F. F. Shape and size optimization of truss structures considering dynamic constraints through modern metaheuristic algorithms. v. 39, n. 10, p. 9458–9467, 2012.

MOHAMED, A. H.; MUTALIB, S.; YUSOFF, M.; RAHMAN, S. A. Modified branch and bound algorithm. *Proceedings of the 8th WSEAS International Conference on Evolutionary Computing*, 2007.

MUSKULUS, M.; SCHAFHIRT, S. Design optimization of wind turbine support structures — a review. *Journal of Ocean and Wind Energy*, v. 1, n. 1, p. 12–22, 2014.

NOCEDAL, J.; WRIGHT, S. J. *Numerical Optimization*. 2nd. ed. New York, USA: Springer, 2006.

OFTADEH, R.; MAHJOOB, M. J.; SHARIATPANAHI, M. A novel meta-heuristic optimization algorithm inspired by group hunting of animals: Hunting search. *Computers and Mathematics with Applications*, v. 60, n. 7, p. 2087–2098, 2010.

OLIVEIRA, M. C. de. Offshore platforms sizing optimization through genetic algorithms. In: DEEP OFFSHORE TECHNOLOGY CONFERENCE - DOT. Perth, Australia, 2008.

PEREZ, R.; BEHDINAN, K. Particle swarm approach for structural design optimization. *Computers and Structures*, p. 1579–1588, 2007.

RAJEEV, S.; KRISHNAMOORTHY, C. S. Discrete optimization of structures using genetic algorithms. *Journal of Structural Engineering*, v. 118, n. 5, p. 1233–1250, 1992.

RAO, S. S. *Engineering optimization : theory and practice*. 4th. ed. Hoboken, New Jersey: John Wiley & Sons Inc., 2009.

RASTI-BARZOKI, M.; HEJAZI, S. R.; MAZDEH, M. M. A branch and bound algorithm to minimize the total weighed number of tardy jobs and delivery costs. *Applied Mathematical Modelling*, v. 37, p. 4924–4937, 2013.

RERE, L. M. R.; FANANY, M. I.; ARYMURTHY, A. M. Simulated annealing algorithm for deep learning. *Procedia Computer Science*, v. 72, p. 137 – 144, 2015.

ROCHA, K. M. *Otimização Topológica de Vigas Metálicas com Aberturas na Alma*. Master Dissertation — Universidade do Estado do Rio de Janeiro, 2017.

RUBINSTEIN, R. Y. Optimization of computer simulation models with rare events. *European Journal of Operations Research*, v. 99, p. 89–112, 1997.

RUBINSTEIN, R. Y. The cross-entropy method for combinatorial and continuous optimization. *Methodology and Computing in Applied Probability*, v. 1, n. 2, p. 127–190, 1999.

RUBINSTEIN, R. Y. Combinatorial optimization, cross-entropy, ants and rare events. *Stochastic Optimization: Algorithms and Applications*, v. 54, p. 303–363, 2001.

RUBINSTEIN, R. Y.; KROESE, D. P. *Simulation and the Monte Carlo Method*. 3rd. ed. Hoboken, New Jersey, USA: Wiley, 2017.

RUBINSTEIN, R. Y.; MELAMED, B. *Modern Simulation and Modeling*. New York: John Wiley & Sons, 1998.

RUBISTEIN, R. Y.; KROESE, D. P. *The Cross-Entropy Method: A Unified Approach to Combinatorial Optimization, Monte-Carlo Simulation, and Machine Learning*. New York, USA: Springer, 2004.

SAITOU, K.; IZUI, K.; NISHIWAKI, S.; PAPALAMBROS, P. A survey of structural optimization in mechanical product development. *Journal of Computing and Information Science in Engineering*, v. 5, n. 3, p. 214–225, 2005.

SAKA, M.; HASANCEBI, O.; GEEM, Z. Metaheuristics in structural optimization and discussions on harmony search algorithm. v. 28, p. 88–97, 2016.

SANDERS, E. D.; AGUILÓ, M. A.; PAULINO, G. H. Multi-material continuum topology optimization with arbitrary volume and mass constraints. *Computer Methods in Applied Mechanics and Engineering*, v. 340, p. 798–823, 2018.

SHANNO, D. F. Conditioning of quasi-newton methods for function minimization. *Mathematics of Computation*, v. 24, n. 111, p. 647–656, 1970.

SHUKLA, P. K.; TIWARI, K. D. Comparing classical generating methods with an evolutionary multi-objective optimization method. *International Conference on Evolutionary Multi-Criterion Optimization*, n. 3, p. 311–325, 2005.

SILVA, G. B. da. *Otimização Tpológica de Estruturas Contínuas considerando incertezas.* Master Dissertation — Universidade do Estado do Paraná, 2016.

SILVA NETO, A. J.; BECCENERI, J. C. *Técnicas de inteligência computacional inspiradas na natureza: Aplicação em problemas inversos em transferência radiativa.* São Carlos, SP: SBMAC, 2009. v. 41.

SILVA NETO, A. J.; SOEIRO, F. J. C. P. The solution of an inverse radiative transfer problem with the simulated annealing and levenberg-marquardt methods. *SBMAC - Serie II*, Rio de Janeiro, Brazil, VII, n. 1, p. 17–30, 2006.

SLAUGHTER, W. S. *The Linearized Theory of Elasticity.* New York, USA: Springer, 2002.

SNYMAN, J. A.; WILKE, D. N. *Practical Mathematical Optimization: Basic Optimization Theory and Gradient-Based Algorithms.* 2nd. ed. New York, USA: Springer, 2018.

SORENSEN, K. Metaheuristics — the metaphor exposed. *International Transactions in Operational Research*, n. 1, 2013.

SOUZA, R. R. de; MIGUEL, L. F. F.; LOPEZ, R. H.; MIGUEL, L. F. F.; TORII, A. J. A procedure for the size, shape and topology optimizationof transmission line tower structures. *Engineering Structures*, v. 111, n. 15, p. 162–184, 2016.

SPENCER, A. J. M. *Continuum Mechanics.* New York, USA: Dover Publications, 2004.

TALISCHI, C.; PAULINO, G. H.; PEREIRA, A.; MENEZES, I. F. M. Polygonal finite elements for topology optimization: A unifying paradigm. *International Journal for Numerical Methods in Engineering (Print)*, v. 82, p. 671–698, 2010.

THEDIN, R.; MENEZES, I. F. M.; PEREIRA, A.; CARVALHO, M. S. Embedding of polytopes for topology optimization. *Journal of the Brazilian Society of Mechanical Sciences and Engineering*, p. 40:57, 2018.

VANDERPLAATS, G. N. Structural optimization-past, present, and future. *AIAA Journal*, v. 20, n. 7, p. 992–1000, 1982.

VANDERPLAATS, G. N. Structural optimization for statics, dynamics and beyond. *Journal of the Brazilian Society of Mechanical Sciences and Engineering*, v. 28, n. 3, p. 316–322, 2006.

VATANABE, S. L.; LIPPI, T. N.; LIMA, C. R. de; PAULINO, G.; SILVA, E. C. N. Topology optimization with manufacturing constraints: A unified projection-based approach. *Advances in Engineering Software*, v. 100, p. 97–112, 2016.

VENKATARAMAN, P. *Applied optimization with MATLAB programming.* New York, USA: John Wiley & Sons, 2002.

WEYLAND, D. A rigorous analysis of the harmony search algorithm: How the research community can be misled by a “novel” methodology. *International Journal of Applied Metaheuristic Computing (IJAMC)*, v. 1, n. 2, p. 50–60, 2010.

YANG, X. S. *Engineering Optimization: An Introduction with Metaheuristic Applications.* Hoboken, New Jersey: John Wiley & Sons, Inc., 2010.

YILMAZ, O. C. *The Optimization of Offshore Wind Turbine Towers Using Passive Tuned Mass Dampers.* Master Dissertation — University of Massachusetts - Amherst, 2014.

YUAN, Y. A new stepsize for the steepest descent method. *Journal of Computational Mathematics*, v. 24, n. 2, p. 149–156, 2006.

ZAVALA, G. R.; NEBRO, A. J.; LUNA, F.; COELLO, C. A. A survey of multi-objective metaheuristics applied to structural optimization. *Structural and Multidisciplinary Optimization*, v. 49, n. 4, p. 537–558, 2014.

ZHANG, X. *Macro-Element approach for topology optimization of trusses using a ground structure method.* Master Dissertation — University of Illinois at Urbana-Champaign, 2014.

ZOHDI, T. I. *A Finite Element Primer for Beginners: The Basics.* 2nd. ed. Cham, Switzerland: Springer, 2018.

APPENDIX A – Parameter analysis - Truss 1

This appendix contains the parameter analysis of the Truss 1 optimization.

A.1 Optimization with yield stress constraint

This section contains the parameter analysis considering yield stress constraint.

In the SQP, a formula for the gradient can be provided (Analytics gradient) or not (Numerical gradient) for parameter analysis. Table 42 shows how the change in the tolerance value affects the processing time and result. Other parameter values are the default of MATLAB.

Table 42 - Values of objective function and Func. Eval. obtained by SQP, not considering buckling, in Truss 1.

	Numerical gradient		Analytics gradient	
`tol`	mass (kg)	Func. Eval.	mass (kg)	Func. Eval.
10^{-2}	9.6	15	9.6	5
10^{-3}	9.6	18	9.6	6
10^{-4}	9.6	18	9.6	6
10^{-6}	9.6	21	9.6	7

The Table 42 shows how informing the gradient is relevant, in this case, when not considering the buckling. The change in the value of `tol` influences in Func. Eval., where decreasing `tol`, increases Func. Eval..

The values for the CE parameters that were used, such as N^s, N^e and `tol`, are the ones that obtained the best result. For the comparative effect, the same values are used for the GA parameters. In this case, Ps and p_e have the same values as N^s and N^e in the parameter analyses. The parameter value are shown in Table 43.

Table 43 - Values of objective function and Func. Eval. obtained by GA for several values of `tol`, p_e and Ps, not considering buckling, in Truss 1.

$Ps = 25$						
p_e	15%		20%		25%	
`tol`	mass (kg)	Func. Eval.	mass (kg)	Func. Eval.	mass (kg)	Func. Eval.
10^{-2}	9.7	1325	9.9	1325	9.8	1325
10^{-3}	9.7	2625	9.7	2625	9.8	2625
10^{-4}	9.6	3925	9.7	3925	9.7	3925
10^{-6}	9.6	11120	9.7	6525	9.7	6525
Ps= 50						
p_e	15%		20%		25%	
`tol`	mass (kg)	Func. Eval.	mass (kg)	Func. Eval.	mass (kg)	Func. Eval.
10^{-2}	10.0	2650	9.9	2650	9.8	2650
10^{-3}	9.9	5250	9.7	5250	9.8	5250
10^{-4}	9.6	7850	9.7	7850	9.7	7850
10^{-6}	9.9	8650	9.7	13050	9.7	8500
$Ps = 100$						
p_e	15%		20%		25%	
`tol`	mass (kg)	Func. Eval.	mass (kg)	Func. Eval.	mass (kg)	Func. Eval.
10^{-2}	9.6	5300	9.7	5300	9.7	5300
10^{-3}	9.7	10500	9.6	10500	9.7	10500
10^{-4}	9.7	17200	9.8	17200	9.6	17200
10^{-6}	9.6	21900	9.6	22700	9.6	20900
$Ps = 150$						
p_e	15%		20%		25%	
`tol`	mass (kg)	Func. Eval.	mass (kg)	Func. Eval.	mass (kg)	Func. Eval.
10^{-2}	9.7	7962	9.7	7962	9.6	7962
10^{-3}	9.7	15750	9.7	15750	9.7	15750
10^{-4}	9.6	23550	9.6	23550	9.6	23550
10^{-6}	9.7	39150	9.6	39150	9.6	39150

In the case shown in Table 43, when the GA parameter values increase, such as Ps and p_e, the solutions found are closer to the optimum; following the solution found by the SQP as a reference. The increase of the `tol` makes the search of the optimal solution more refined, increasing the Func. Eval., while the increase of p_e does not seems to influence.

Notice that in Table 44, increasing `tol` greatly increases the function evaluations (Func. Eval.), and also taking the objective function closer to the SQP result, which is used as reference, making the method more refined. In general, with the increase in the value of N^e, N^s, `tol` and ϱ, more function evaluations are required. Just as in the same way of GA, by increasing the values of the parameters the solution of the CE gets closer to the solution of the SQP.

Table 44 - Values of objective function and Func. Eval. obtained by CE for several values of `tol`, ϱ and N^s, not considering buckling, in Truss 1.

$N^s = 25$						
ϱ	15%		20%		25%	
`tol`	mass (kg)	Func. Eval.	mass (kg)	Func. Eval.	mass (kg)	Func. Eval.
10^{-2}	10.1	150	10.2	175	9.7	225
10^{-3}	9.7	275	9.7	325	9.7	400
10^{-4}	9.7	400	9.7	525	9.7	550
10^{-6}	9.7	575	9.7	750	9.7	950
$N^s = 50$						
ϱ	15%		20%		25%	
`tol`	mass (kg)	Func. Eval.	mass (kg)	Func. Eval.	mass (kg)	Func. Eval.
10^{-2}	9.9	400	9.9	500	9.9	500
10^{-3}	9.8	550	9.9	750	9.9	750
10^{-4}	9.8	800	9.7	1100	9.7	1150
10^{-6}	9.7	1250	9.7	1800	9.7	1800
$N^s = 100$						
ϱ	15%		20%		25%	
`tol`	mass (kg)	Func. Eval.	mass (kg)	Func. Eval.	mass (kg)	Func. Eval.
10^{-2}	9.8	700	10.0	700	9.8	900
10^{-3}	9.7	1100	9.7	1200	9.7	1500
10^{-4}	9.6	1600	9.6	1700	9.6	2400
10^{-6}	9.6	2600	9.6	2600	9.6	3900
$N^s = 150$						
ϱ	15%		20%		25%	
`tol`	mass (kg)	Func. Eval.	mass (kg)	Func. Eval.	mass (kg)	Func. Eval.
10^{-2}	9.7	1200	9.8	1200	9.7	1350
10^{-3}	9.7	1800	9.7	1950	9.6	2400
10^{-4}	9.6	2550	9.6	2850	9.7	3150
10^{-6}	9.6	3900	9.6	4200	9.6	4950

A.2 Optimization with yield stress and buckling limit constraints

This section has the parameter analysis considering, in the optimization problem, yield stress and buckling constraints.

Considering buckling, the value for parameter analyses in the SQP of the Truss 1 are in the Table 45. In this case, providing the gradient of the objective function and constraints made the Func. Eval. somewhat smaller. The change in the value of `tol` matters. The parameter analyses done in GA and CE, changing parameter values, are shown in the Table 46 and Table 47.

Table 45 - Objective functions optimal obtained by SQP considering buckling in Truss 1.

	Numerical gradient		Analytics gradient	
`tol`	mass (kg)	Func. Eval.	mass (kg)	Func. Eval.
10^{-2}	13.9	28	13.9	16
10^{-3}	13.9	31	13.9	17
10^{-4}	13.9	37	13.9	19
10^{-6}	13.9	40	13.9	20

Table 46 - Values of objective function and Func. Eval. obtained by GA for several values of `tol`, p_e and Ps considering buckling in Truss 1.

$Ps = 50$						
p_e	20%		25%		30%	
`tol`	mass (kg)	Func. Eval.	mass (kg)	Func. Eval.	mass (kg)	Func. Eval.
10^{-2}	14.0	2650	18.7	2662	14.6	5450
10^{-3}	14.1	5262	14.1	5250	14.2	5262
10^{-4}	13.9	5262	14.7	8500	13.9	5274
10^{-6}	14.3	13600	14.3	20250	14.0	13050
$Ps = 100$						
p_e	20%		25%		30%	
`tol`	mass (kg)	Func. Eval.	mass (kg)	Func. Eval.	mass (kg)	Func. Eval.
10^{-2}	14.0	31400	13.9	17600	14.4	31500
10^{-3}	14.6	16000	14.1	32100	13.9	10512
10^{-4}	14.0	10512	14.0	37000	13.9	10512
10^{-6}	14.0	39000	14.0	15712	13.9	15712
$Ps = 150$						
p_e	20%		25%		30%	
`tol`	mass (kg)	Func. Eval.	mass (kg)	Func. Eval.	mass (kg)	Func. Eval.
10^{-2}	14.1	47550	14.4	27450	14.0	7950
10^{-3}	14.0	15762	14.4	46800	13.9	27150
10^{-4}	14.3	57900	14.0	59850	14.3	28200
10^{-6}	14.2	23572	13.9	23578	14.3	40350
$Ps = 200$						
p_e	20%		25%		30%	
`tol`	mass (kg)	Func. Eval.	mass (kg)	Func. Eval.	mass (kg)	Func. Eval.
10^{-2}	14.5	32200	14.3	62400	18.5	10612
10^{-3}	13.9	21012	14.3	62400	14.4	63000
10^{-4}	14.0	21012	13.9	21024	13.9	21012
10^{-6}	14.3	76800	14.6	46000	13.9	31412

Table 47 - Objective functions optimal obtained by CE for several values of `tol`, ϱ and N^s, not considering buckling, in Truss 1.

$N^s = 50$						
ϱ	20%		25%		30%	
`tol`	mass (kg)	Func. Eval.	mass (kg)	Func. Eval.	mass (kg)	Func. Eval.
10^{-2}	14.5	1200	14.4	1400	14.6	1550
10^{-3}	14.2	2100	14.0	2300	14.2	2700
10^{-4}	14.1	3050	14.0	3400	14.0	3850
10^{-6}	14.3	4750	14.3	5400	14.0	5700
$N^s = 100$						
ϱ	20%		25%		30%	
`tol`	mass (kg)	Func. Eval.	mass (kg)	Func. Eval.	mass (kg)	Func. Eval.
10^{-2}	14.9	2500	14.7	2800	14.6	3800
10^{-3}	14.5	4200	14.4	4700	14.4	6400
10^{-4}	14.4	5700	14.0	6700	14.0	8500
10^{-6}	14.2	9500	14.0	10400	14.1	13800
$N^s = 150$						
ϱ	20%		25%		30%	
`tol`	mass (kg)	Func. Eval.	mass (kg)	Func. Eval.	mass (kg)	Func. Eval.
10^{-2}	14.2	4050	14.2	4650	14.1	5550
10^{-3}	14.2	6750	14.1	7650	14.1	9300
10^{-4}	14.2	9600	14.1	10800	14.0	12900
10^{-6}	14.1	15300	14.1	17400	14.0	21450
$N^s = 200$						
ϱ	20%		25%		30%	
`tol`	mass (kg)	Func. Eval.	mass (kg)	Func. Eval.	mass (kg)	Func. Eval.
10^{-2}	14.0	5600	14.2	6400	14.2	7400
10^{-3}	14.0	9200	14.2	10400	14.2	1220
10^{-4}	14.0	13000	14.0	15000	14.2	18200
10^{-6}	14.0	21600	14.0	25200	14.2	29400

When buckling is considered, the convexity of the optimization problem is lost, giving rise to local extrema. Due to the non-convexity of the problem, the influence of changing the parameter values becomes more random. Note that by increasing `tol`, there is a large increase in the function evaluations (Func. Eval.).